Ozone Response to Emission Reductions in the Southeastern United States

Charles L. Blanchard[1], George M. Hidy[2]

[1] Envair, Albany, CA, 94706, USA

5 [2] Envair/Aerochem, Placitas, NM, 87043, USA

Correspondence to: Charles L. Blanchard (cbenvair@pacbell.net)

Abstract. Ozone (O_3) formation in the southeastern U.S. is studied in relation to nitrogen oxide (NO_x) emissions using long-term (1990s – 2015) surface measurements of the Southeastern Aerosol Research and Characterization (SEARCH) network, U.S. Environmental Protection Agency (EPA) O_3 measurements, and EPA Clean Air Status and Trends Network (CASTNet)
10 nitrate deposition data. CASTNet data show declining wet and dry nitrate deposition since the late 1990s, with total (wet plus dry) nitrate deposition fluxes decreasing linearly in proportion to reductions of NO_x emissions by ~60% in Alabama and Georgia. Annual nitrate deposition rates at Georgia and Alabama CastNet sites correspond to 30% of Georgia emission rates and 36% of Alabama emission rates, respectively. The fraction of NO_x emissions lost to deposition has not changed over time. SEARCH and EPA CASTNet sites exhibit downward trends in mean annual nitric acid (HNO_3) concentrations. Mean annual
15 total oxidized nitrogen (NO_y) mixing ratios at SEARCH sites declined in proportion to NO_x emission reductions. Annual 4th-highest daily peak 8-hour O_3 mixing ratios at EPA monitoring sites in Georgia, Alabama, and Mississippi exhibit statistically-significant ($p < 0.0001$) linear correlations with annual NO_x emissions in those states between 1996 and 2015. The annual 4th-highest daily peak 8-hour O_3 mixing ratios are declining toward non-zero values of ~45 – 50 ppbvand monthly O_3 maxima declined at rates averaging ~1 – 1.5 ppbv y^{-1}. Observed relationships of O_3 to NO_z (NO_y – NO_x) suggest increasing
20 responsiveness of O_3 to NO_x over the study period.

1 Introduction

Ozone (O_3) is a well-known and important product of photochemical processes in the troposphere involving nitric oxide (NO), nitrogen dioxide (NO_2), and volatile organic compounds (VOCs). Ozone is of broad interest for its adverse effects on humans and ecosystems, as reflected by regulation through the U.S. Clean Air Act (e.g., U.S. EPA, 2014; 2015a).
25 Regulatory actions address extreme O_3 mixing ratios: the U.S. National Ambient Air Quality Standard (NAAQS), currently 70 ppbv, is applicable to the annual 4th-highest daily eight-hour maxima averaged over three-year periods (U.S. EPA, 2015b; 2015c). By the early 1990s, U.S. emission control efforts began to focus on nitrogen oxides ($NO_x = NO + NO_2$) in addition to VOCs (NRC, 1991). O_3 management has generally relied on precursor reduction requirements estimated from models that integrate descriptions of non-linear chemical and atmospheric processes (e.g., Seigneur and Dennis, 2011), and guidance has

also derived from so-called "observation-based" models linking O_3 and its precursors based on chemical reactions that are believed to drive ambient mixing ratios (e.g., NARSTO, 2000; Schere and Hidy, 2000).

Most of the work developing an observational basis for O_3-precursor chemistry derives from field campaigns, sometimes focusing on urban conditions. Short-term data are available from aircraft flights, for example, or summer field measurements made at a variety of locations. Such studies usually are limited to a month or two of intense sampling. One example in the southern U.S. is the 1990 ROSE Experiment at Kinterbish, a rural, forested state park in western Alabama (Frost et al., 1998). This summer study of rural O_3 at low anthropogenic VOC and low NO_x mixing ratios provided important insights into rural O_3 formation (Trainer et al., 2000). Other examples of short-term campaigns across the U.S. and elsewhere are reviewed in Solomon et al. (2000). More recent field studies include New England in 2002 (e.g., Griffin et al., 2004; Kleinman et al., 2007), Texas in 2006 (e.g., Berkowitz et al., 2005; Neuman et al., 2009), the mid-Atlantic region in 2011 (He et al., 2013), California in 2010 (Ryerson et al., 2013), Colorado in 2012 and 2014 (e.g., McDuffie et al., 2016), and the southeastern U.S. in 2013 (e.g., Neuman et al., 2016; Warneke et al., 2016). These campaigns and accompanying analyses of O_3 production and accumulation typically address summer, which historically has the strongest photochemical activity. However, strong photochemical O_3 production can occur under special circumstances in winter (e.g., Schnell et al., 2009).

Accounting for an O_3 background is important. O_3 background is associated with biogenic influence, large-scale transport, or the potential influence of the upper atmosphere (e.g., stratospheric intrusions, especially during spring) (e.g., Lin et al., 2012; Langford et al., 2015). The nature and magnitude of background O_3 remain an active area of research in the U.S. and Europe (Naja et al., 2003; Solberg et al., 2005; Ordóñez et al., 2007; Cristofanelli and Bonasoni, 2009; Arif and Abdullah, 2011; Zhang et al., 2011; Wilson et al., 2012). Hidy and Blanchard (2015) discuss definitions of continental and regional background O_3. For this study, we adopt a definition of "background" that includes both the non-anthropogenic component and the southeastern regional component (Section 4.4.1).

Field studies have provided observational evidence of non-linearity in O_3-NO_z relationships (e.g., Trainer et al., 1993; Kleinman et al., 1994; Trainer et al., 1995; Hirsch et al., 1996; Frost et al., 1998; Kasibhatla et al., 1998; Nunnermacker et al., 1998; St. John et al., 1998; Sillman et al., 1998; Zaveri et al., 2003; Griffin et al., 2004; Travis et al., 2016). Long-term, post-1990s data are widely available for O_3 and NO_2 but detailed observations of total oxidized nitrogen (NO_y) and VOC, and especially their component species, are typically lacking (e.g., Hidy and Blanchard, 2015). One of the longest records of urban and suburban data, comprising a series of short-term campaigns as well as continuous measurements, is from southern California. This region exemplifies a photochemically active urban regime. An analysis of multi-decadal (since the 1960s) data by Pollack et al. (2013) reveals how changes in atmospheric chemical reactions have contributed to the observed reductions of O_3 in southern California since 1973. Long-term (more than one decade) measurements characterizing O_3 and NO_y relationships in both urban and rural conditions are less common.

The photochemical regime in the Southeast represents humid subtropical conditions with urban emissions yielding elevated O_3 levels superimposed on a general regional background (Chameides and Cowling, 1995). The EPA O_3 and deposition data provide a regional basis for characterizing trends since the early 1980s (U.S. EPA 2016a; 2016b). In addition, the Southeastern

Aerosol Research and Characterization (SEARCH) project (Hansen et al., 2003; Hidy et al., 2014) provides measurements that can be used to investigate changes in O_3 production resulting from changes in anthropogenic emissions in the southeastern U.S. The SEARCH network of eight sites began with the Southeastern Oxidant Study (SOS) (Chameides and Cowling, 1995; Meagher et al., 1998) rural locations, which were near (1) Centreville, AL, ~85 km southwest of Birmingham, (2) at Yorkville, GA, ~60 km northwest of Atlanta, GA and (3) at Oak Grove, MS, ~40 km southeast of Hattiesburg, MS, and 75 km north of Gulfport, MS, on private land within the confines of the Desoto National Forest (Hansen et al., 2003). Measurements of some gas-phase species began at these rural sites in 1992, thus providing a rural data record of over 20 years. Beginning in 1999, SEARCH added five sites in metropolitan Atlanta, GA, Birmingham, AL, Pensacola, FL, and Gulfport, MS.

Our goal for this study is to extend earlier analyses of the photochemical response of O_3 to precursors through 2014, emphasizing relationships between O_3 and NO_y. We first summarize relevant O_3 photochemistry to provide a context for the observational analysis. We then describe trends in emissions and ambient pollutant concentrations, and discuss O_3, NO_z, and HNO_3 observations at the SEARCH sites. Blanchard et al. (2014) previously explained the majority (66 - 80%) of the day-to-day variations in daily peak 8-hour average O_3 at SEARCH sites during March – October of 2002 - 2011 using meteorological variables coupled with ambient measurements of O_3 precursors (NO, NO_2; limited measurements of VOCs) and NO_x photochemical reaction products (NO_z) and a statistical model. The previous analyses are extended here for data through 2014 to understand ongoing and potential future O_3 changes in relation to changes in ambient NO_z and HNO_3 mixing ratios in the southeastern U.S.

2 Ozone-Nitrogen Oxide Chemistry

2.1 Key Atmospheric Reactions Linking O_3 with NO_x

Net tropospheric O_3 accumulation occurs when sunlight acts on VOC and NO_x emissions and the O_3 production rate exceeds O_3 loss (Trainer et al., 2000). Tropospheric O_3 mixing ratios are affected by solar intensity, chemical formation and loss (e.g., deposition) rates of O_3, the rate of dispersion of O_3 and its precursors, meteorological factors, vertical entrainment and transport of plumes. NO_2 forms rapidly by reaction of NO with O_3 and photolysis of NO_2 produces O_3, yielding steady-state mixing ratios of NO, NO_2, and O_3 in the absence of other species as expressed by the photostationary state, or Leighton relationship (Seinfeld, 1986).

In the troposphere, NO_2 also forms by reaction of NO with peroxy (HO_2) and alkyl peroxy (RO_2) free radical species, which derive in turn from the reaction of VOCs with hydroxyl (HO), HO_2, RO_2, and alkyl radicals (Seinfeld, 1986). Radical production from VOCs creates a pathway for conversion of NO to NO_2 that does not consume O_3 (Atkinson, 2000), which then leads to higher O_3 mixing ratios.

O_3 accumulation is typically associated with high solar radiation intensity and temperatures favoring atmospheric reactions, lower wind speeds, and high anthropogenic emission rates (NARSTO, 2000). O_3 accumulation requires NO mixing ratios exceeding approximately 10 to 30 pptv (Atkinson, 2000; Logan, 1985), along with the presence of HO_2 and RO_2 radicals that

react with NO to form NO_2. The former conditions are normally met in urban air; NO_x mixing ratios are much lower under typical conditions in rural southeastern areas, but still well above 30 pptv (e.g., Hudman et al., 2007; Travis et al., 2016). Under these conditions, the O_3 photochemical production rate is proportional to the ambient NO multiplied by the sum of HO_2 and RO_2 radical mixing ratios, where the latter are weighted by their rates of reaction with NO (Trainer et al., 2000). Field studies
5   show that observed rates of rural O_3 production are proportional to the rate of oxidation of NO_x. Where VOCs are present for radical production and NO_x is rate-limiting (Trainer et al., 2000), regional O_3 production can be expressed in terms of the derivative $d[O_3]/d[NO_x]$, denoted the O_3 production efficiency (OPE) (Liu et al.,1987). OPE is understood as the number of molecules of O_3 formed per molecule of NO_x oxidized and OPE increases as NO_x mixing ratios decrease (Liu et al., 1987; Trainer et al., 2000). OPE reflects the mean number of NO-NO_2 cycles occurring, in which each photolysis of one NO_2
10   molecule generates one O_3 molecule until that NO_2 molecule is oxidized to nitric acid (HNO_3) or to other species such as peroxyacetylnitrate (PAN). NO_x reaction products, including HNO_3 and PAN, comprise NO_z. For chemical reactions, the quantity $d[O_3]/d[NO_z]$ is equivalent to $d[O_3]/d[NO_x]$ but with opposite sign, and has therefore been used to estimate OPE; limitations due to confounding influences of emissions, transport, and deposition are discussed in Sections 4.3 and 4.4.

Empirically, the slope of a linear fit of afternoon O_3 (or $O_x = O_3 + NO_2$) versus NO_z has been used to estimate OPE (e.g.,
15   Trainer et al., 1993; Pollack et al., 2013). This estimate is subject to certain limitations because it does not explicitly account for: (1) day-to-day variability in "old" (baseline or regional background) O_3 mixing ratios, (2) mixing of air masses having different emission histories, (3) rapid loss of HNO_3 (primarily through dry deposition, but also through gas-to-particle conversion) (Trainer et al., 2000), and (4) regeneration of NO_2 from PAN and certain other species. Because PAN regenerates NO_2, it can serve as a reservoir rather than a true NO_2 sink (Singh and Hanst, 1981; Singh, 1987). In contrast, HNO_3 largely
20   terminates the cycling between NO and NO_2. Therefore, the relative yields of PAN and HNO_3 are of importance. Despite such limitations in using measurements to quantify OPE, data from field studies have been used since the 1990s to determine upper bounds for OPE and the results have continued to appear in the literature as an indicator of relevance to O_3 chemistry (e.g., Berkowitz et al., 2005; Neuman et al., 2009; Kim et al., 2016). Investigators caution that field measurements reveal the net of production and loss, which potentially overestimates actual OPE by factors of 3 to 6 due to rapid chemical and deposition
25   losses of HNO_3 and other NO_z species (e.g., Trainer et al., 2000). Additional discussion is found in Section 4.4.

In southern California, changes in the relative proportions of NO_x-oxidation products have occurred and are thought to be instrumental in driving the rapid rates of O_3 decline in that area (Pollack et al., 2013). These results indicate that measurements of HNO_3 or PAN are needed to identify important changes in chemical pathways.

2.2 National O_3 Response to Emission Reductions

30   Between 1980 and 2013, the national average of the annual 4th-highest peak daily 8-hour O_3 mixing ratios, a metric relevant to the U.S. O_3 NAAQS, declined by 33% (U.S. EPA, 2015d) as national VOC and NO_x emissions decreased by 53% and 52%, respectively (U.S. EPA, 2015e). Across the U.S. and on multiple spatial scales from continental to urban, annual 4th-highest daily peak 8-hour O_3 mixing ratios between 1980 and 2013 show a statistically significant ($p < 0.05$) linear fit to either annual

average or to 98th percentile daily maximum hourly NO_2 mixing ratios; regression slopes are less than 1:1 and intercepts are in the range of 30 to 50 ppbv O_3 (Hidy and Blanchard, 2015). Proportionalities between O_3 and NO_2 that are less than 1:1 are expected, and the observed intercept terms are approximately consistent with typical O_3 mixing ratios of ~20 – 50 ppbv observed at remote monitoring sites (Oltmans et al., 2008; 2013; U.S. EPA, 2012; Fiore et al., 2014; Lefohn et al., 2010; 2014;

5   Cooper et al., 2012; 2014).

Although nonlinearity of O_3 production and accumulation with respect to ambient VOC and NO_x is well established (Lin et al., 1988), a tendency toward linearity is expected at sufficiently low NO_x mixing ratios. As an example, the O_3 photochemical production rate during June 1990 at Kinterbish, AL was approximately linear over a range of ambient NO_x from 0.1 to 2 ppbv (Trainer et al., 2000). Observed O_3 extrema can also exhibit an apparent linear or near-linear response to ambient NO_x mixing

10   ratios if the extrema consistently fall within the lower-right quadrant (NO_x-sensitive regime) of an O_3-VOC-NO_x diagram, a concise graphical representation first established empirically from southern California data and later generated using the Empirical Kinetics Modeling Approach (EKMA) (illustrated in Hidy and Blanchard, 2015). The O_3-VOC-NO_x diagram has been adopted by many investigators for displaying the output of box models (e.g., Fujita et al., 2003; 2015) and grid-based photochemical models (e.g., Reynolds et al., 2003; 2004).

15   Southern California historically has exhibited the highest peak O_3 mixing ratios in the U.S. since the 1960s. Because of high ambient O_3 and precursor mixing ratios there and the complexity of the relationships of O_3 with NO_x and VOC, some investigators have described southern California O_3 and precursor trends in terms of percentage changes. For example, Pollack et al. (2013) report that peak 8-hour O_3 mixing ratios in southern California declined exponentially over time at a rate of 2.8% per year between 1973 and 2010, thus decreasing O_3 levels by approximately a factor of three. This rate of O_3 decline exceeds

20   rates occurring in other metropolitan areas (Hidy and Blanchard, 2015). O_3 extrema in southern California decreased along with declining mixing ratios of ambient VOCs and NO_x (7.3% yr^{-1} and 2.6% yr^{-1}, respectively, 1960 – 2010) and declining ratios of VOC/NO_x (4.8% yr^{-1}) (Pollack et al., 2013). The rates of atmospheric oxidation of NO_x increased over time and changes in NO_x oxidation reactions increasingly favored production of HNO_3, a NO_x reaction product associated with radical termination and quenching of the O_3 formation cycle (Pollack et al. 2013). To our knowledge, changes in the relative

25   proportions of atmospheric reaction products accounting for rapid rates of O_3 reduction have not been reported for locations other than southern California.

3 Methods

3.1 Emissions and Ambient Air Quality Measurements

Air quality monitoring data were obtained from the EPA Air Quality System (AQS) data archives for all sites in Georgia,

30   Alabama, and Mississippi (U.S. EPA, 2016a). Daily measurement values (i.e., peak daily 8-hour O_3 mixing ratio) as well as annual summary statistics (e.g., maxima, annual averages) were acquired. We obtained deposition data from the two EPA Clean Air Status and Trends Network (CASTNet) monitoring sites located within the study region: Sand Mountain, AL (125

km ENE of the SEARCH site at Centreville) and Georgia Station, GA (102 km SE of the SEARCH site at Yorkville) (U.S. EPA, 2016b).

Annual, state-level emission trends data were obtained from U.S. EPA (2016c; 2016d), Xing et al. (2013), and Hidy et al. (2014). Comparability of inventories is discussed in the supplementary material (Figure S1). Because the EPA trend inventory

5 utilized different methods for estimating mobile source emissions prior to 2002 compared with 2002 and later years, we combined EPA trend estimates for 2002 – 2016 with the 1996 - 2001 emission estimates of Hidy et al. (2014), which are consistent with more recent EPA methods (supplementary material).

Hourly measurements of gases (NO, NO_2, NO_y, HNO_3, and O_3) were obtained from SEARCH public archives (Atmospheric Research and Analysis [ARA], 2017). All parameters measured at the sites are calibrated and audited to conventional reference

10 standards, as described in ARA (2015). Network operations, sampling, and measurement methods are documented in Hansen et al. (2003; 2006); see also Table S1. The network consisted of eight extensively instrumented monitoring sites located in the southeastern U.S. along the Gulf of Mexico and inland (Figure S2): Pensacola, Florida (PNS) and Gulfport, Mississippi (GFP), urban coastal sites (~ 5 km and 1.5 km from the shoreline, respectively); Pensacola – outlying (aircraft) landing field (OLF) and Oak Grove, Mississippi (OAK), non-urban coastal sites near the Gulf (~20 km and 80 km inland, respectively); Atlanta,

15 Georgia – Jefferson Street (JST) and North Birmingham, Alabama (BHM), urban inland sites; and Yorkville, Georgia (YRK) and Centreville, Alabama (CTR), non-urban inland sites. PNS, OAK, and GFP were closed at the end of 2009, 2010, and 2012, respectively. SEARCH site locations are described in detail, including discussion of possible emission influences, in Hansen et al. (2003) and Hidy et al. (2014). SEARCH VOC data are available for JST as daily data from 1999 through 2008, and U.S. EPA VOC measurements are available for YRK as summer hourly data and as 24-hour samples collected every sixth day

20 throughout the year (Blanchard et al., 2010). EPA VOC samples are also available for three other sites in the Atlanta area; only one of these additional sites reported data through 2014.

SEARCH meteorological parameters and gases are sampled at a height of 10 meters, characteristic of lower troposphere mixing ratios near the surface (Hansen et al., 2003; Hansen et al., 2006; Edgerton et al., 2007; Saylor et al., 2010). Gas and meteorological measurements commenced in 1992 at the rural sites of CTR, OAK, and YRK. The measurements at rural

25 SEARCH sites included O_3, NO, and NO_y beginning in 1992, and NO_2 and HNO_3 measurements began in 1996. Consistent measurement methods have been utilized for all gases except NO_2. NO_2 measurements commenced network-wide in 2002, and three NO_2 measurement methods have been employed during the network operations (Table S3). All three methods are NO_2-specific, differing primarily in the light source used for photolysis of NO_2. The NO_2 data exhibit consistency with NO and NO_y measurements but with some variations occurring during specific years (e.g., 2001 and 2002, Figure S3). Because

30 changes in NO_2 measurement methods could affect the computed NO_z (NO_y – NO – NO_2), we repeat some data analyses using HNO_3 in place of NO_z. As noted, HNO_3 data also provide useful insight into NO_2 termination reactions. HNO_3 measurements are the difference between NO_y and denuded NO_y (Table S1; Hansen et al., 2006). The SEARCH measurements of NO_y were designed to capture particulate nitrate and organic nitrates, as well as NO, NO_2, HNO_3, and other oxidized nitrogen species. The NO_y sampler derives from the instrument identified in Williams et al. (1998) as "ESE", which was one of five instruments

for which measurements of NO_y reproduced the sum of separately measured NO_y species. Additional testing in 2013 showed that SEARCH NO_y measurements agreed with the sum of measured mixing ratios of NO, NO_2, HNO_3, particulate nitrate, alkyl nitrates, and peroxy–alkyl nitrates (Hidy et al., 2014).

Trace gas calibrations were done daily for O_3 and every third day for other gases. Reported detection limits (Table S1) are 0.05 – 0.1 ppbv for oxidized nitrogen species and 1 ppbv for O_3 (Hansen et al., 2003; 2006). NO_2 measurement uncertainties are estimated as ~30% prior to 2002 and ~10% after 2002 (Hansen et al., 2006). Measurement uncertainties are estimated to be 10% or less for other oxidized nitrogen species and 5% or less for ozone (2 sigma in all cases). Propagation of errors indicates corresponding 2-sigma measurement uncertainties averaging 0.5 ppbv for mid-afternoon NO_z (< 0.1 ppbv for NO_z < 1 ppbv) and 0.16 for the ratio NO_z/NO_y.

3.2 Data Analysis

Multiple methods were employed to characterize the variability of ambient O_3 and NO_y mixing ratios. Analyses of seasonal variability used data from all months of each year. Diurnal hourly average mixing ratios were computed by year to characterize patterns of temporal change and to identify hours associated with O_3 maxima. Observed slopes of regressions of O_3 versus NO_z were computed as previously done in measurement studies using afternoon O_3 and NO_z data (Trainer et al., 1993; Kleinman et al., 1994; Trainer et al., 1995; Hirsch et al., 1996; Kasibhatla et al., 1998; Nunnermacker et al., 1998; St. John et al., 1998; Sillman et al., 1998; Zaveri et al., 2003; Griffin et al., 2004; Travis et al., 2016). Because past studies have examined O_3 formation in photochemically aged air (i.e., at locations distant from fresh emissions, where atmospheric reactions have acted on emissions from earlier times) during summers (e.g., Trainer et al., 1993), our analyses focus on the months of June and July to select weeks nearest maximum solar radiation (~ -20 days, + 40 days). Additional analyses were carried out for other months to facilitate comparisons across seasons. As for earlier studies, the calculations are based on afternoon times, using hourly values starting at 2 p.m. local standard time to represent the daily peak O_3 after morning production and before mixing ratios decline with decreasing photochemical reaction in later afternoon. In addition to characterizing O_3/NO_z and its change with time, corresponding supporting analyses are presented for O_3/HNO_3. As a supplemental analysis, rates of maximum diurnal increase of O_3 and HNO_3 during late morning and early afternoon were computed for comparison of ΔO_3 with ΔHNO_3.

4 Results and Discussion

4.1 Trends

Hidy et al. (2014) report a 63% reduction of NO_x emissions in the southeastern U.S. between 1996 and 2014. The largest NO_x emission changes in the Southeast occurred between 2007 and 2009 due to reductions of emissions from electric generating units (EGUs) and from diesel engine vehicles, and were accompanied by more gradual year-to-year reductions of gasoline-

engine mobile-source NO_x emissions (de Gouw et al., 2014; Hidy et al., 2014). NO_x emission reductions led to approximately proportional responses of mean ambient NO_y and NO_z mixing ratios at SEARCH sites (Hidy et al., 2014).

The EPA CASTNet data show wet and dry nitrate deposition since the late 1990s declining at rates of ~5% per year (-0.045 ± 0.005 and -0.056 ± 0.005 y^{-1}), nearly identical to NO_x emission changes of -0.046 ± 0.001 and -0.051 ± 0.003 y^{-1} (Figure 1).

5 Total (wet plus dry) nitrate deposition fluxes decreased linearly in proportion to reductions of NO_x emissions in Alabama and Georgia (Figure 1). Linear regression slopes indicate that the annual nitrate deposition fluxes at the Georgia and Alabama CASTNet sites correspond to 30% of Georgia emissions and 36% of Alabama emissions on an annual and statewide basis (Figure 1). Emissions are not spatially homogeneous and deposition losses likely vary with distance from emission sources. The two sites are situated differently in relation to metropolitan areas, possibly affecting deposition fluxes; Sand Mountain

10 (SND) is northeast of Birmingham and Georgia Station (GAS) is south of Atlanta. The linearity and statistical significance of the regressions indicates that the fraction of NO_x emissions lost to deposition has not changed over time (ratios of annual deposition-to-state-emissions varied without trend from 0.23 – 0.34 at GAS and 0.30 – 0.45 at SND). Mean annual SEARCH NO_y mixing ratios at rural CTR and YRK declined at ~5 – 7% y^{-1} (Figure S4). SEARCH and EPA CASTNet sites exhibit downward trends in mean annual HNO_3 concentrations of ~9 – 11% y^{-1} and ~6 – 7% y^{-1}, respectively (Figure S4). Ambient

15 NO_y and HNO_3 trends are not statistically different from state-level NO_x emission trends.

Annual 4th-highest daily peak 8-hour O_3 mixing ratios at compliance monitoring sites in Georgia, Alabama, and Mississippi exhibit statistically-significant ($p < 0.0001$) linear correlations with annual NO_x emissions in those states between 1996 and 2015 (Figure 2), qualitatively consistent with past work indicating that high O_3 would respond to reductions of NO_x emissions (Chameides and Cowling, 1995; Jacob et al., 1995; Kasibhatla et al., 1998). Intersite differences in the annual 4th-highest daily

20 peak 8-hour O_3 mixing ratios have decreased (Figure 2), consistent with an analysis of data from a larger number of U.S. and European locations (Paoletti, et al., 2014). The annual 4th-highest daily peak 8-hour O_3 mixing ratios are declining toward non-zero values, as indicated by the statistically-significant ($p < 0.0001$) intercepts of ~45 – 50 ppbv (Figure 2). SEARCH data are used to characterize the southeastern O_3 response to emission changes in greater detail. Between 1999 and 2014, the highest peak daily 8-hour O_3 mixing ratios occurring each month (monthly O_3 maxima) declined at all SEARCH sites at statistically

25 significant ($p < 0.01$) rates averaging ~1 – 1.5 ppbv y^{-1} (Figure 3). These declines are comparable to the trend in the 95th percentile summer peak daily 8-hour O_3 mixing ratios in the southeastern U.S. of ~ -0.8 to -1.8 ppbv yr^{-1} reported by Lin et al. (2017), with downward trends occurring in other seasons as well. The observed SEARCH O_3 trends are also consistent with other analyses of North American observations (e.g., Chan, 2009; Lefohn et al., 2010; Paoletti, 2014; Simon et al., 2015) and with the trends occurring at EPA monitors in the Southeast (Figure 2). Both EPA (Figure 2) and SEARCH (Figure 3) data

30 suggest that O_3 mixing ratios increased during the 1990s, then began declining. The SEARCH trends are compared with emission changes in the Southeast, and with emission and O_3 trends in southern California, in Table S2.

More complete understanding of regional O_3 trends requires consideration of both regional emission changes and possible changes in background O_3. Multiple definitions of the term "background O_3" may be found in the literature, including global background, continental background, non-anthropogenic background, and regional background, among others. For the O_3

trends shown in Figures 2 and 3, the most relevant consideration is the amount of O_3 transported into the study domain across upwind boundaries (denoted here as regional background or transported O_3). The percentage reductions of O_3 are larger if transported O_3 can be estimated and subtracted from observed O_3 mixing ratios, and this adjustment potentially provides a better assessment of the effects of regional emission reductions on the fraction of O_3 that is manageable by means of local and

5   regional emission control measures. For example, Parrish et al. (2017a) report that the O_3 enhancement above background in Southern California decreased by 4.5% yr^{-1}, which is larger than the unadjusted O_3 decline of 2.8% y^{-1} given by Pollack et al. (2013). Similarly, rates of decline in southeastern U.S. O_3 are larger if regional background O_3 is considered (Table S2).

Defining and estimating regional background (or transported) O_3 are challenging. We interpret the intercepts in Figure 2 as indicators of mean O_3 levels that would occur on days with weather conducive to high O_3 in the absence of NO_x emissions

10   from AL and GA sources, i.e., as estimators of O_3 transported into the region from outside the study domain (as discussed subsequently, multi-day carryover of local and regional emissions during stagnation events could also affect intercepts and slopes). Days with weather that is not conducive to high O_3 would have different levels of transported O_3. The statistically-significant slopes in Figure 2 indicate O_3 enhancements that are attributable to AL-GA emissions, except as noted next, and a comparison of the O_3 decline to intercept-corrected O_3 would then reveal the proportionality between AL-GA emissions and

15   AL-GA O_3 enhancements over O_3 originating outside the study domain (i.e., in excess of regional background O_3). Although the ~30 – 35% O_3 declines are less than proportional to the ~60% decrease in NO_x emissions, the decline in the median O_3 is ~60% if the 50 ppbv intercept shown in Figure 2 is subtracted from the O_3 mixing ratios.

If the amount of O_3 that has been transported from upwind regions has been changing over time, e.g., declining as NO_x emissions and ambient O_3 decline in adjacent regions, the slopes shown in Figure 2 would reflect changes in both the O_3 that

20   originated upwind and in the O_3 enhancements attributable to AL-GA emissions, confounding attribution. Related studies do not provide consistent evidence for a trend, either upward or downward, in regional background O_3 in the southeastern U.S. For example, baseline O_3 concentrations in air flowing into Texas from the Gulf of Mexico during May through October did not change significantly between 1998 and 2012 (Berlin et al., 2013). Mean regional background O_3 mixing ratios were 48 ppbv to 59 ppbv in the Houston, TX, area on days with O_3 levels exceeding the NAAQS, which includes O_3 contributions from

25   transport to the area from other regions of the U.S. (Berlin et al., 2013). Observed trends in the 5th percentile O_3 have previously been used as indicators of changes in either regional or continental background O_3 (e.g., Wilson et al., 2012). The 5th percentile peak daily 8-hour O_3 mixing ratios decreased during summer at rural sites throughout the southeastern U.S. between 1988 and 2014 (Lin et al., 2017). By this measure, regional background O_3 levels were not increasing in the southeastern U.S. during our study period.

30   Large-scale transport affecting O_3 in the boundary layer and at the surface is a function of altitude. For example, during June 2013, anthropogenic emissions and long-range transport (long-range tropospheric + stratospheric) O_3 each accounted for about 40% (15 – 20 ppbv each) of model-predicted O_3 below 1 km altitude at Huntsville, AL, while long-range transport accounted for ~80% of model-predicted O_3 above 4 km altitude (Johnson et al., 2016). This variation of source contributions with altitude provides an opportunity to differentiate between emission-related and transport-related trends derived from vertical soundings

of upper-air O_3 mixing ratios. Using ozonesondes that are generally launched on a weekly schedule, vertical O_3 mixing ratio profiles have been determined by the University of Alabama in Huntsville, Alabama, since 1999 (Newchurch et al., 2003; Johnson et al., 2016; University of Alabama, 2017; NOAA, 2017). We obtained these ozonesonde data (n = 940 days) and identified the following statistically significant trends in the lower layers that are relatively more influenced by local and

5   regional emissions according to Johnson et al. (2016): -0.25 ± 0.11 ppbv y^{-1} (p < 0.05) in daily measurements at 0.5 km, -0.40 ± 0.10 ppbv y^{-1} (p < 0.0001) at 1 km (daily), -0.42 ± 0.09 ppbv y^{-1} (p < 0.0001) at 2 km (daily), and -0.57 ± 0.13 ppbv y^{-1} in monthly averages of O_3 measurements made throughout the interval 1 – 2 km (p < 0.001). At higher altitudes where Johnson et al. (2016) predicted that long-range transport is the dominant source of O_3, no trends occurred: 0.06 ± 0.08 ppbv y^{-1} (p > 0.1) at 4 km (daily) and 0.09 ± 0.19 ppbv y^{-1} (p > 0.1) at 8 km (daily).

10   Global background is one component of regional background and trends in global background are expected to contribute to trends in regional background. Lin et al. (2017) show that rising NO_x emissions in Asia have increased modeled North American background O_3 levels (based on model simulations with zero North American emissions) by ~0.2 ppbv yr^{-1} in the southeastern U.S. in summer, which is a small effect even when cumulated over 20 years in comparison with the ~25 ppbv reduction in the median annual 4th-highest peak daily 8-hour O_3 shown in Figure 2. Multiple studies have demonstrated

15   increasing trends in global background O_3 mixing ratios (Ordóñez et al., 2007; Oltmans et al., 2008; Arif and Abdullah, 2011; Wilson et al., 2012). Parrish et al. (2017a) report that the highest O_3 design values (the 3-year running mean of the annual 4th-highest peak daily 8-hour O_3 mixing ratio) in Southern California are converging toward of limit of 62.0 ± 1.9 ppb, which they identify as the O_3 design values that would result from U.S. background O_3 concentrations. Parrish et al. (2017b) report decreasing O_3 transported across the Pacific into the western U.S. after 2000. As noted, regional background O_3 in the

20   southeastern U.S. does not appear to be trending either upward or downward, even though trends in background O_3 have been established in other areas or globally.

In the southeastern U.S., the simple conceptual model of O_3 transported into a study region across upwind boundaries is incomplete. High O_3 typically occurs during multi-day stagnation episodes, which are associated with the presence of high barometric pressure over the domain and limited transport (Blanchard et al., 2013). Transport distances determined from 24-

25   hour back-trajectory computations are less then 300 km for the highest decile O_3 (Blanchard et al., 2013). Mean 24-hour transport distances are less than 350 km during June and less than 380 km during July (Blanchard et al., 2014). These distances are approximately equivalent to distances from Birmingham to Mobile, AL, or from Atlanta to Savannah, GA. Local and regional emissions can accumulate over multiple days and potentially could contribute to observed O_3 concentrations (e.g., aloft) that are considered as regional background. In contrast to emissions originating upwind, carryover from emission sources

30   within the study domain is a component of manageable O_3.

4.2 Seasonal Variations of O_3, NO_y, NO_z, HNO_3, and VOCs

The seasonal oscillations of monthly O_3 maxima in the Southeast are coupled to local or regional meteorology, solar radiation, and emissions (e.g., Blanchard et al., 2013; 2014; Hidy et al., 2014). Variations of daily maximum temperature and mid-day relative humidity (RH)are associated with variations of daily peak 8-hour O_3 mixing ratios by ~ ±30 percent from mean peak 8-hour O_3 mixing ratios, after also accounting for variations of other meteorological factors (Blanchard et al., 2014). Air mass back trajectories originating from the south (~ 150 to 200 degrees) exhibit peak 8-hour O_3 that is ~5 – 10 percent lower than average; daily peak O_3 decreases as 24-hour back trajectory distances increase from zero to ~600 km, consistent with association of higher O_3 concentrations with air mass stagnation rather than transport (Blanchard et al., 2013; 2014). At SEARCH sites, the monthly O_3 maxima (highest daily peak 8-hour O_3 each month) and mean daily peak 8-hour O_3 mixing ratios typically occurred in summer months, especially inland, and declined more than other monthly maxima (Figures 3 and 4). Summer means were not always higher than spring averages, especially at rural and coastal sites and during more recent years (Figure 4). Roughly constant winter monthly peak 8-hour maxima of ~40 ppbv occurred throughout the period of record (Figure 3). The seasonal variability of the highest peak daily 8-hour O_3 therefore declined over time (see also Table S3). Similar results were found for monthly means of hourly measurements, discussed in Section 4.3 on diurnal variations. Other recent studies have reported decreasing seasonal variability of O_3 across the U.S. using data from large numbers of monitoring sites (Chan, 2009; Chan and Vet, 2010; Cooper et al., 2012; Paoletti et al., 2014; Simon et al., 2015). Declines in seasonal variability are thought to result from changing rates of O_3 formation as precursor emissions have declined, or from increasing influence of intercontinental background O_3, not from changes in seasonal variations of temperature and other meteorological factors (Chan, 2009; Cooper et al., 2012; Simon et al., 2015).

The SEARCH data indicate that seasonal variations occur in ambient O_3, NO_y, NO_z, HNO_3, and the ratio of NO_z/NO_y (Figure 5). Seasonal variations of temperature and other meteorological factors are known to cause seasonal variations of O_3 and NO_y species concentrations. The monthly average NO_z and HNO_3 mixing ratios indicate that active photochemical processing of NO_x occurs during well more than half the year in the warm climate of the southeastern U.S.The effects of VOC species on O_3 formation depend on both their ambient concentrations and their reactivities. To describe VOC variations at sites with long-term VOC measurements, we use isoprene data as an indicator of biogenic VOCs and toluene as an indicator of anthropogenic VOCs (nominally emitted as a gasoline vapor). The importance of isoprene emissions for O_3 production in the southeastern U.S. is well established (e.g., Chameides et al., 1988; Chameides and Cowling, 1995; Frost et al., 1998; Starn et al., 1998; Wiedinmyer et al., 2006; Zhang et al., 2014; Lin et al., 2017). We also consider other reactive VOC species of interest, including α-pinene (biogenic) as well as ethylene and xylenes (anthropogenic). Summer (June – August) months exhibit elevated ambient mixing ratios of rural and urban isoprene, typically about 5 – 10 ppbC, that are one to two orders of magnitude greater than those occurring between October and April (Figure 6). Transitions between low and high ambient isoprene mixing ratios occur in mid-May and mid-September in northern Georgia (Figure 6). Annual mean isoprene mixing ratios were relatively constant, ~2.5 – 3 ppbC, between 1998 and 2014. Biogenic VOCs, primarily isoprene, represent ~20% of the VOC

reactivity at JST, ~30% at South Dekalb (SDK, located in metropolitan Atlanta ~16 km southeast of JST), and ~50% at YRK, averaged over all samples collected between 1999 and 2007 (Blanchard et al., 2010a). Through precursor interactions, seasonal variations in isoprene mixing ratios are expected to affect seasonal variations in O_3 mixing ratios and production rates.

5 Mean mixing ratios of ethylene and aromatic compounds vary substantially between urban and rural sites and exhibit less, and a different, seasonal variation than does isoprene, peaking in the fall rather than in the summer (compare Figures 6, S5, S6). Daily average mixing ratios of toluene, xylenes, and ethylene decline over the years, consistent with regulatory reductions of anthropogenic VOC emissions (Figures S5, S6). Seasonal variations in ambient mixing ratios and trends in the anthropogenic emissions of aromatic compounds are expected to influence O_3 mixing ratios and production in urban settings (rural anthropogenic VOC mixing ratios are lower but detectable).

10 The 24-hour average VOC mixing ratios are of somewhat limited value for showing the influence of VOCs on O_3 formation and accumulation. VOC influence is dependent on NO_x mixing ratios, which vary depending on proximity to emission sources and time of day. Meteorological variability, including diurnal and day-to-day changes in temperature, vertical mixing, cloud cover, photolysis, and air mass transport, further obscures the quantitative effects of VOCs on seasonal and interannual variations of O_3. Influences of anthropogenic VOCs at SEARCH sites have previously been reported (Blanchard et al., 2010b;

15 2014) and are not analyzed beyond this summary.

4.3 Diurnal Variations of O_3, NO_y, NO_z, and HNO_3

Summer (June – August) mean O_3 mixing ratios exhibit characteristic nocturnal minima and mid-day (noon to 4 p.m., midpoint ~ 2 p.m.) maxima at all SEARCH sites (Figure 7). This diurnal pattern remained essentially the same at both the urban and rural sites from 1999 through 2014, but the daytime maxima decreased. Between 1999 and 2014, the summer mean mid-day

20 maxima declined by ~30 ppbv at all sites, while nocturnal means exhibited variable responses (Figure 7). Similar diurnal variations occur throughout the year, with smaller decreases in the mean mid-day O_3 maxima occurring during seasons other than summer (Figures S7 – S9). By the end of the study period, diurnal O_3 profiles were higher during spring (March through May) than summer at the rural sites (CTR and YRK, Figures S7 and S8), consistent with the reduction in summer mean monthly daily peak 8-hour O_3 averages (Figure 4). Decreasing summer diurnal mean NO_y, HNO_3, and NO_z mixing ratios were

25 also observed, with a general flattening of the profiles and with the times of maxima remaining consistent (Figures S10-12). O_3 changes are discussed in relation to changes in NO_y and NO_z in Section 4.4, with emphasis on summer and additional consideration of spring months.

4.4 Observed Relationships between O_3 and NO_z

As discussed above, O_3 mixing ratios vary seasonally and diurnally in response to variations in emissions, weather, background

30 O_3, and other factors. To reduce the influence of seasonal and diurnal variability, this section focuses on mixing ratios of NO_z, HNO_3, and O_3 at 2 p.m. during June and July. Both temperature and solar radiation are typically high during June and July, and multi-day stagnation events occur frequently in association with high barometric pressure (Blanchard et al., 2013).

Exceptions exist during the passage of frontal systems (Blanchard et al., 2013; Figure S13). The 2 p.m. hour has the highest, or close to highest, average hourly O_3 for all sites and years (Figure 7). The atmosphere is well-mixed by mid-day. Over the range of ambient mixing ratios observed across 15 years, the June-July 2 p.m. O_3 values are distinctly nonlinear in relation to ambient NO_z and HNO_3 mixing ratios (Figure 8). More variability is evident at urban sites than at rural sites, consistent with influence of urban NO_x and perhaps VOC emissions on O_3. The nonlinearity indicated in Figure 8 is also evident when the data are restricted to days having the highest peak daily 8-hour O_3 mixing ratios (Figure S14).

4.4.1 Linear Models

Linear regressions are fit to the afternoon data by year, as shown in Figure 9 for 2013 and in Table S4 for all years. During multi-week periods within any summer, all sites exhibit near-linear relationships of mid-day O_3 to NO_z. Because the ranges of NO_x and NO_z mixing ratios within each year are limited, year-specific relationships are close to linear and linear models are statistically significant. Steeper slopes at rural sites than at urban sites in Figure 9 suggest that either more O_3 molecules formed per molecule of NO_x consumed in rural locales than in urban areas, or that greater losses of NO_z occurred at the rural sites, as discussed below. At all sites, similar results are obtained for regressions of O_x ($O_3 + NO_2$) vs NO_z compared with O_3 vs NO_z (Figure 9, caption). At 2 p.m., rural O_3 mixing ratios are nearly identical with O_x mixing ratios and with other metrics (e.g., O_3 – [NO_y – NO]) (Figure S15). At urban sites, 2 p.m. NO_2 mixing ratios are non-negligible, but this difference alters the intercepts rather than the slopes of the regressions of O_x vs NO_z compared with O_3 vs NO_z (Figure 9). As previously noted (Figure S13), even during the two-month periods that we analyzed, the weather is not always conducive to O_3 formation and such days could influence the observed slopes and intercepts. However, regression results restricted to days with weather that favors O_3 formation (as defined in Figure 9) do not differ from the unrestricted regressions.

Plotting the year-specific (June – July) computed regression slopes versus mean June – July 2 p.m. NO_z shows significant increases over time as ambient NO_z mixing ratios have decreased, subject to year-to-year variability (Figure 10, Table S4). Similar urban-rural differences and patterns of increasing regression slopes are also observed when data are restricted to March and April (spring) at YRK and JST (Figure S16). The results for spring show more variability than the summer year-specific linear models. One key difference between spring and summer days is that cumulative solar radiation between sunrise and 2 p.m. is greater on summer days than on spring days, presumably fostering greater photochemical extent of reaction and accumulation of O_3 during summer.

The regression slopes determined from 2 p.m. data could reflect day-to-day differences in transported O_3 if background O_3 is consistently higher on high-O_3 days than on low-O_3 days and NO_z is not (in contrast, random variations in day-to-day background O_3 and NO_z would introduce variations, or scatter, around the regression lines). We checked for an effect of this type by repeating the analyses using differences in mixing ratios. Two sets of difference-based regressions are used: (1) the differences between 2 p.m. and 10 a.m. hourly measurements, and (2) the differences between 11 a.m. and 10 a.m. hourly measurements. The differences are computed for each day to minimize or eliminate the unknown day-specific background levels, and are then used in the regressions. These hours were selected to focus on times of day when the atmosphere is well-

mixed. The morning rise in mixing heights is expected to contribute to increases in the mixing ratios of secondary species as aged air aloft is incorporated into the mixed layer. The most rapid rates of increase in diurnally-averaged O_3, NO_z, and HNO_3 values occur between ~8 a.m. and 12 noon local time (Figures 7, S8 – S9). By mid- to late-morning hours during summer, considerable vertical entrainment has occurred, and subsequent changes in the mixing ratios of secondary species likely reflect

5   same-day atmospheric chemical reactions. Computing afternoon – morning differences and late morning – mid-morning differences helps account for day-to-day variations in regional background O_3, but also introduces higher relative uncertainties due to poorer statistical fit because four measurements (two differences) are used in the regressions. Results for all three approaches are tabulated in Table S5, by site and year. Like the regressions based on 2 p.m. measurements, the difference-based regressions indicate slope increases over time (Table S5, Figures S17 – 19). The best statistical fits are for the regressions

10   using non-differenced afternoon data. The difference-based regressions exhibit lower slopes than the non-differenced afternoon regressions, which could be due to lesser statistical fit, or to better accounting for variations in regional background O_3, or to a combination of these factors. The difference-based regressions suggest that slopes increased from less than 5:1 in the late 1990s and early 2000s to values between 5:1 and 10:1 after 2010 (Figures S17 – S19; Table S5). These values are consistent with our previous results in which O_3-NO_z relationships were determined while accounting for day-to-day variations in

15   meteorology, which indicated that within the range of 1 to 5 ppbv NO_z, JST, YRK, and CTR O_3/NO_z slopes were 3.5, 5.0, and 7.1, respectively, for measurements made during March – October of 2002 - 2011 (Blanchard et al., 2014). Although the difference-based regressions in principle account for the possibility that background O_3 is consistently higher on high-O_3 days than on low-O_3 days, uncertainties about background variability remain and are discussed below in relation to the intercepts. A second potential effect on the temporal changes in the regression slopes could be due to changes in NO_2 measurement

20   methods, previously described; this possibility was checked by using regressions of O_3 vs. HNO_3 (Figure S20). The results indicate that the relationship in Figure 10 is not an artifact of changes in NO_2 measurement methods. The record is more complete for the regressions of O_3 vs. HNO_3, because the HNO_3 measurements were made over a longer time than the NO_2 measurements (and the latter are needed for computing NO_z). As shown for YRK, the year-specific slopes of 2 p.m. O_3 vs. NO_z and for O_3 vs. HNO_3 each increased substantially after about 2008 (Figures 10, S20). The O_3 vs. NO_z and O_3 vs. HNO_3

25   regression slopes tend to level out after 2011, and possibly decrease somewhat, but variability is too high to project beyond the observed data ranges (Figures 10, S20). Similar results are obtained for spring for JST and YRK (Figures S21 and S22). Our increases in year-specific slopes of O_3 versus NO_z potentially could be due to increasing losses of NO_z species, especially HNO_3, over the long-term SEARCH record. As previously noted, however, the CASTNet data show declining rates of both wet and dry nitrate deposition since the late 1990s, with no change in the ratio of deposition to emissions (Figure 1). Therefore,

30   the long-term slope increases cannot be attributed to increasing deposition losses of HNO_3 (whether absolute or fractional). Qualitatively, the CASTNet data suggest that the observed slopes would likely be at least a factor of two smaller if adjusted for deposition losses. This adjustment would be comparable to the 1990s studies discussed in Section 4.4.2.In Figure 9, the intercepts of year-specific regressions for 2013 approach 20 ppbv O_3, which could be interpreted as a regional background O_3 level relatively unaffected by local chemistry. These values are lower than those in Figure 2 and lower than the estimated range

of 48 ppbv to 59 ppbv for air transported into the Houston area. They are also lower than modeled western non-U.S.-anthropogenic regional background O_3 levels of ~ 40 – 50 ppbv (Lefohn et al., 2014; Dolwick et al., 2015) but are consistent with model estimates of non-U.S.-anthropogenic background O_3 less than ~30 ppbv in Atlanta (Lefohn et al., 2014). Since regression intercepts restricted to days with weather that favors O_3 formation do not differ much from the intercepts of the

5   unrestricted regressions (Figure 9), our low intercepts for recent years do not appear to be linked to meteorological conditions that specifically favor O_3 loss over formation. However, when considered over the full set of years, the O_3-NO_z relationships on the highest O_3 days differ from those on lager subsets of the data (Figure S14). Possibly, the intercept terms cannot be fully interpreted without additional consideration of O_3 carryover in multiday episodes, as previously noted. The intercept terms for earlier years are higher than for later years; for example, the intercepts for the YRK regressions range from 27 ± 3 to 42 ± 4

10   ppbv prior to 2009 (for all but two of these years, intercepts are $36 - 38$ ppbv). The intercept terms for earlier years are consistent with 1997 – 2006 eastern U.S. summer baseline O_3 levels (32 ± 12 ppbv in the absence of continental influences) reported by Chan and Vet (2010).

Higher intercepts during early years could be due to fitting a linear regression to the upper portion or the mid-range of the nonlinear relationship between O_3 and NO_z, as shown in Figures 8 and S14. The nonlinearity and the downward trends in mean

15   NO_z and HNO_3 mixing ratios mean that slopes of regressions computed at higher mean NO_z and HNO_3 mixing ratios should not be extrapolated beyond their range of applicability to the y-intercept. Alternatively, the trend toward lower intercepts could reflect declining mixing ratios upwind of the study sites, consistent with documented long-term reductions of ambient O_3 mixing ratios throughout the U.S. (e.g., Chan and Vet, 2010; Lefohn et al., 2010; Paoletti, 2014; Simon et al., 2015; Hidy and Blanchard, 2015). As previously discussed, however, regional background O_3 in the southeastern U.S. does not appear to be

20   trending either upward or downward,

4.4.2 Comparisons with Observed and Modeled Regression Slopes and OPE

The preceding section shows that the slopes of the regressions of O_3 versus NO_z increased over time, a result that holds when based on differences between hourly concentrations as well as on non-differenced afternoon mixing ratios. The increasing slopes appear to indicate that relationships between O_3 and NO_z changed over time, yet the physical processes associated with

25   the changes remain ambiguous. The data were selected to represent periods that have consistent weather from day to day to minimize the influence of meteorological variability, and regressions of subsets of the data yield slopes and intercepts comparable to those based on all days of June and July. Although slopes could be affected by changes in O_3 concentrations transported into the region, as previously discussed, other studies do not indicate that trends have occurred in regional background O_3. However, the O_3 decreases that have occurred in the region (Figures 2 and 3) could not have occurred if NO_x

30   emissions declined by ~60%, or ~5% per year over 20 years (Figure 1; Hidy et al., 2014), but O_3 formation rates increased by factors of ~3 to 4 (Figure 10). Even the factor of two increase in the slopes of the difference-based regressions, from ~5:1 to ~10:1 are difficult to reconcile with the magnitudes of the NO_x emission reductions and ambient O_3 decreases. The regression slopes are nonetheless consistent with related studies when a basis for comparison exists.

The SEARCH observed afternoon slope values of ~5:1 prior to 2003 – 2007 are comparable to, or lower than, similar regression results obtained in studies during the 1990s, which showed observed summer slope values of 11:1 in rural Georgia in 1991 (Kleinman et al., 1994), 8.5:1 at rural eastern sites (Trainer et al., 1993), 7:1 near Birmingham, AL in 1992 (Trainer et al., 1995), 5.7:1 near Nashville, TN in 1995 (Sillman et al., 1998), and 4.7:1 near Nashville, TN, in 1999 (Zaveri et al., 2003), and

5   to modeling results and observations with composite regression slope values of 6.7 and 7.6, respectively, within the afternoon planetary boundary layer in the eastern U.S. during the summer of 2002 (Godowitch et al., 2011) The SEARCH regression slope values prior to 2003 – 2007 are, as expected, higher than other 1990s values that were corrected for deposition losses, which, for example, yielded adjusted estimated OPE values between 3:1 and 5:1 near Nashville in 1995 (Nunnermacker et al., 1998; St John et al., 1998; Sillman et al., 1998). Our higher observed slope values after 2010 are consistent with aircraft

10   measurements made in the Southeast in August and September 2013, which show O_x (= O_3 + NO_2) versus NO_z slope of 17.4, and they are also consistent with model calculations, which show slopes of 14.1 to 16.7 (Travis et al., 2016). Consistent with our regressions, Travis et al. (2016) did not adjust for variations in background O_3 and NO_z. For comparability, we note that our O_3 versus NO_z regression slopes were 13.1 to 18.8 (± 1.2 to 1.4) in June and July, 2013, at three of four sites (25.7 ± 2.8 at the fourth site, which is the most rural in character) and our O_x versus NO_z slopes were 12.0 to 18.9 (± 1.2 to 1.4) at three

15   of the four sites (25.8 ± 2.8 at the fourth site). The increase in recently observed slope values that we report is therefore supported by the 2013 data of Travis et al. (2016). Our apparently high regression slope values are also consistent with observation-based OPE that averaged 12.9 in ship plumes and 33.5 in assumed background marine air, as reported by Kim et al. (2016) using data from a 2002 study of ship emission plumes off the coast of southern California, though the specific conditions associated with these two studies are different from ours and thus limit the applicability of the comparisons.

20   The increase in regression slopes with decreasing ambient NO_x and NO_z is also consistent with computations by Liu et al. (1987), which showed increasing OPE as NO_x declines. The numerical results of the modeling calculations by Liu et al. (1987) are specific to the modeled conditions, which represented complete oxidation of VOCs over a period of months. However, increases in model-predicted NO_x OPE with declining NO_x results from multiple factors, such as radical reactions involving VOCs and NO_x, that are pertinent to other situations (Lin et al., 1988).

25   In contrast to southern California, where Pollack et al. (2013) reported a shift from PAN to HNO_3 production with no change in OPE, the SEARCH data do not definitively show a changing fraction of HNO_3 relative to NO_y. Increasing formation of PAN (which regenerates NO_2) and decreasing formation of HNO_3 (which terminates cycling between NO and NO_2) could facilitate O_3 accumulation as ambient NO_x and NO_z mixing ratios continue to decline. Since the long-term SEARCH data record does not include measurements of PAN, this possible effect could not be investigated.

30   **5 Implications**

The trends in, and relationships between, O_3 and NO_y species provide some insight into the potential for future O_3 changes in the southeastern U.S. The post-1990s O_3 trend provides one guide to future average rates of O_3 reduction in the sense that the rates of O_3 reduction during the next decade are unlikely to deviate dramatically from those of the recent past.

Anthropogenic NO_x and VOC emissions are each expected to continue to decline. Anthropogenic VOC mixing ratios have declined since 1999, but natural components such as isoprene and terpene mixing ratios have remained relatively constant (Figure 6; Blanchard et al., 2010a; Hidy et al., 2014), leaving ambient VOC levels increasingly dependent on biogenic emissions. Evidence suggests that O_3 formation in the SEARCH region will move toward more NO_x sensitive conditions with

5   continued decreases in NO_x and anthropogenic VOC emissions, coupled with high levels of natural VOC emissions in the region. This anticipated emission reduction path should reinforce the O_3-NO_z relationships and the interpretation presented here.

6 Conclusions

Summer O_3 mixing ratios declined along with decreasing emissions in the southeastern U.S. between 1999 and 2014. The

10   seasonal variability of the highest peak daily 8-hour O_3 mixing ratios also declined over time: summer monthly O_3 maxima declined more than other monthly maxima, while winter monthly maxima of ~40 ppbv occurred throughout the period of record. The seasonal differences in the past O_3 response to NO_x emission reductions could have implications for future O_3 management if spring and autumn O_3 maxima fail to decline and thereby become a focus of concern that merits attention comparable to summer O_3 maxima.The observed relationships of O_3 to NO_z, which is the product of reactions involving NO_x,

15   are nonlinear and suggest increasing responsiveness of O_3 to NO_x over the study period. In addition, changes in the relative importance of chemical reactions that yield HNO_3 compared with PAN are likely to play a role in altering O_3 accumulation.

Data Availability

The   SEARCH   data   are   available   at
https://www.dropbox.com/sh/o9hxoa4wlo97zpe/AACbm6LetQowrpUgX4vUxnoDa?dl=0. EPA data are available at

20   http://aqsdr1.epa.gov/aqsweb/aqstmp/airdata/download_files.html and at https://www.epa.gov/castnet.

Author Contributions

C. L. B. and G. M. H. designed the study and wrote the manuscript. C. L. B. carried out the statistical analyses.

Competing Interests

The authors declare that they have no conflict of interest.

Acknowledgments

The authors thank Atmospheric Research and Analysis, Inc. for collecting, validating, and providing SEARCH data, and J. Jansen for managing the SEARCH study. Funding for the SEARCH network was provided by Southern Company with contributions from the Electric Power Research Institute. Southern Company provided partial financial support for analysis of
5   SEARCH data. We are indebted to these sponsors for supporting this unique long-term measurement program.

References

Arif, N. L. and A. M. Abdullah: Ozone pollution and historical trends of surface background ozone level: a review, World Applied Sciences Journal, 14 (Exploring Pathways to Sustainable Living in Malaysia: Solving the Current Environmental Issues), 31-38, 2011.

10   Atkinson, R.: Atmospheric chemistry of VOCs and NO_x, Atmos. Environ., 34, 2063 – 2101, 2000.

Atmospheric   Research   and   Analysis   (ARA): https://www.dropbox.com/sh/o9hxoa4wlo97zpe/AACbm6LetQowrpUgX4vUxnoDa?dl=0 (last access April 24, 2017), 2017.

Blanchard, C.L., S. Tanenbaum, G. Hidy, R. Rasmussen, and R. Watkins: NMOC, ozone and organic aerosol in the southeastern states, 1999-2007. 1. Spatial and temporal variations of NMOC mixing ratios and composition in Atlanta,

15   Georgia, Atmos. Environ., 44, 4827-4839, 2010a.

Berlin, S. R., A. O. Langford, M. Estes, M. Dong, and D. D. Parrish: Magnitude, decadal changes and impact of regional background ozone transported into the greater Houston, Texas area, Environ. Sci. Technol, 47(24), 13985-13992, doi:10.1021/es4037644, 2013.

Blanchard, C. L., G. M. Hidy, and S. Tanenbaum: NMOC, ozone, and organic aerosol in the southeastern states, 1999-2007:

20   2. Ozone trends and sensitivity to NMOC emissions in Atlanta, Georgia. Atmos. Environ., 44, 4840 – 4849, doi:10.1016/j.atmosenv.2010.07.030, 2010b.

Blanchard, C. L., G. M. Hidy, S. Tanenbaum, E. S. Edgerton, and B. E. Hartsell: The Southeastern Aerosol Research and Characterization (SEARCH) study: Spatial variations and chemical climatology, 1999 – 2010, J. Air Waste Manage. Assoc., 63, 260-275, doi:10.1080/10962247.2012.749816, 2013.

25   Blanchard, C. L., S. Tanenbaum, and G. Hidy: Ozone in the southeastern United States: an observation-based model using measurements from the SEARCH network, Atmos. Environ., 48, 192-200, 2014.

Chameides, W., Lindsay, R., Richardson, J., and Kiang, C.: The role of biogenic hydrocarbons in urban photochemical smog: Atlanta as a case study, Science, 24, 1473–1475, 1988.

Chameides, W. and E. Cowling: The State of the Southern Oxidants Study: Policy Relevant Findings in Ozone Pollution

30   Research, 1988-1994, Southern Oxidant Study, College of Forest Resources, North Carolina State University, Raleigh, NC, 1995.

Chan, E.: Regional ground-level ozone trends in the context of meteorological influences across Canada and the eastern United States from 1997 to 2006, J. Geophys. Res. Atmos., 114, D05301, doi:10.1029/2008JD010090, 2009.

Chan, E. and R. J. Vet, R. J.: Baseline levels and trends of ground level ozone in Canada and the United States, Atmos. Chem. Phys., 10, 8629-8647, doi:10.5194/acp-10-8629-2010, 2010.

5   Cooper, O., R-S. Gao, D. Tarasick, T. Leblanc, and C. Sweeney: Long-term ozone trends at rural ozone monitoring sites across the United States, 1990-2010, J. Geophys. Res. Atmos., 117, D22307, 2012.

Cooper. O., D. Parrish, J. Ziemke, N. Balashov, M. Cupeiro, I. Galbally, S. Gilge, I. Horowitz, N. Jensen, J. Larmarque, N. Naik, S. Oltmans, J. Schwab, D. Shindell, A. Thompson, V. Thouret, Y. Wang, and R. Zhinden: Global distribution and trends of tropospheric ozone: an observation-based review, Elementa, 2, 1-28, doi:10.12952/journalelementa.000029, 2014.

10 Dolwick, P., F. Akhtar, K. R. Baker, N. Possiel, and H. Simon: Comparison of background ozone estimates over the western United States based on two separate model methodologies, Atmos. Environ, 109, 282-296, http://dx.doi.org/10.1016/j.atmosenv.2015.01.005, 2015.

Cristofanelli, P. and P. Bonasoni: Background ozone in the southern Europe and Mediterranean area: influence of the transport processes, Environ. Pollut., 157 (5), 1399-1406, doi.org/10.1016/j.envpol.2008.09.017, 2009.

15 Edgerton, E. S., R. D. Saylor, B. E. Hartsell, J. J. Jansen, and D. A. Hansen: Ammonia and ammonium measurements from the southeastern United States, Atmos. Environ., 41(16), 3339-3351, 2007.

Fiore, A., J. T. Oberman, M.Y. Lin, L. Zhang, O.E. Clifton, D. J. Jacob, V. Naik, L. W. Horowitz, J. P. Pinto, and G. Milly: Estimating North American background ozone in U.S. surface air with two independent global models: variability, uncertainties, and recommendations, Atmos. Environ., 96, 284-300, 2014.

20 Frost, G. J., M. Trainer, G. Allwine, M. P. Buhr, J. G. Calvert, C. A. Cantrell, F. C. Fehsenfeld, P. D. Goldan, J. Herwehe, G. Hubler, W. C. Kuster, R. Martin, R. T. McMillen, S. A. Montzka, R. B. Norton, D. D. Parrish, B. A. Ridley, R. E. Shetter, J. G. Walega, B. A. Watkins, H. H. Westberg, and E. J. Williams: Photochemical ozone production in the rural southeastern United States during the 1990 Rural Oxidants in the Southern Environment (ROSE) program, J. Geophys. Res. Atmos., 103(D17), 22491-22508, 1998.

25 Fujita, E., W. Stockwell, D. Campbell, R. Keisslar, and D. Lawson: Evolution of the magnitude and spatial extent of the weekend ozone effect in California's South Coast Air Basin, 1981-2000, J. Air Waste Manage. Assoc., 53, 802-815, 2003.

Fujita, E., D. E. Campbell, W. Stockwell, E. Saunders, R. Fitzgerald, and R. Perea: Projected ozone trends and changes in the ozone-precursor relationship in the South Coast Air Basin in response to varying reductions of precursor emissions, J. Air Waste Manage. Assoc., 66(2), 201 – 214, 2015.

30 Godowitch, J.M., R. C. Gilliam, and S. T. Rao: Diagnostic evaluation of ozone production and horizontal transport in a regional photochemical air quality modeling system, Atmos. Environ., 45 (24) 3977-3987, 2011.

de Gouw, J. A., D. D. Parrish, G. J. Frost, and M. Trainer: Reduced emissions of CO_2, NO_x, and SO_2 from U.S. power plants owing to switch from coal to natural gas with combined cycle technology, Earth's Future, 2, 75-82, doi: 10.1002/2013EF000196, 2014.

Griffin, R. J., C. A. Johnson, R. W. Talbot, H. Mao, R. S. Russo, Y. Zhou, and B. C. Sive: Quantification of ozone formation metrics at Thompson Farm during the New England Air Quality Study (NEAQS) 2002, J. Geophys. Res. Atmos., 109(D24), D24302, doi:10.1029/2004JD005344, 2004.

Hansen, D.A., E. S. Edgerton, B. E. Hartsell, J. J. Jansen, G. M. Hidy, K. Kandasamy, and C. L. Blanchard: The Southeastern Aerosol Research and Characterization Study (SEARCH): 1. Overview, J. Air Waste Manage. Assoc., 53, 1460-1471, 2003.

Hansen, D. A., E. Edgerton, B. Hartsell, J. Jansen, H. Burge, P. Koutrakis, C. Rogers, H. Suh, J. Chow, B. Zielinska, P. McMurry, J. Mulholland, A. Russell, and R. Rasmussen: Air quality measurements for the aerosol research and inhalation epidemiology study, J. Air Waste Manage. Assoc., 56, 1445-1458, 2006.

He, H., L. Hembeck, K. M. Hosley, T. P. Canty, R. J. Salawitch, and R. R. Dickerson: High ozone concentrations on hot days: The role of electric power demand and NO_x emissions, Geophys. Res. Lett., 40, 5291-5294, doi:10.1002/grl.50967, 2013.

Hidy, G. M. and C. L. Blanchard: Precursor reductions and ground-level ozone in the continental U.S., J. Air Waste Manage. Assoc., 65(10), 1261 – 1282, doi: 10.1080/10962247.2015.1079564. http://dx.doi.org/10.1080/10962247.2015.1079564 (last access August 2, 2017), 2015.Hidy, G., C. Blanchard, K. Baumann, E. Edgerton, S. Tanenbaum, S. Shaw, E. Knipping, I. Tombach, J. Jansen and J. Walters: Chemical climatology of the southeastern United States, 1999-2013, Atmos. Chem. Phys., 14, 11893-11914, 2014.

Hirsch, A. I., J. W. Munger, D. J. Jacob, L. W. Horowitz, and A. H. Goldstein: Seasonal variation of the ozone production efficiency per unit NO_x at Harvard Forest, Massachusetts, J. Geophys. Res. Atmos., 101(D7), 12659-12666, doi:10.1029/96JD00557, 1996.

Hudman, R.C., D. J. Jacob, S. Turquety, E. M. Leibensperger L. T. Murray, S. Wu, A. B. Gilliland, M. Avery, T. H. Bertram, W. Brune, R. C. Cohen, J. E. Dibb, F. M. Flocke, A. Fried, J. Holloway, J. A. Neuman, R. Orville, A. Perring, X. Ren, G. W. Sachse, H. B. Singh, A. Swanson, and P. J. Wooldridge: Surface and lightning sources of nitrogen oxides over the United States: Magnitudes, chemical evolution, and outflow, J. Geophys. Res. Atmos., 112, D12S05, doi:10.1029/2006JD007912, 1997.

Jacob, D. J., L. W. Horowitz, J. W. Munger, B. G. Heikes, R. R. Dickerson, R. S. Artz, and W. C. Keene: Seasonal transition from NOx- to hydrocarbon-limited conditions for ozone production over the Eastern United States in September, J. Geophys. Res. Atmos., 100 (D5), 9315- 9324, 1995.

Johnson, M., S. Kuang, L. Wang, and M. Newchurch: Evaluating summer-time ozone enhancement events in the southeast United States, Atmosphere, 7, 108, doi:10.3390/atmos7080108, 2016.

Kasibhatla, P., W. L. Chameides, R. D. Saylor, and D. Olerud: Relationships between regional ozone pollution and emissions of nitrogen oxides in the eastern United States, J. Geophys. Res. Atmos., 103(D17), 22663-22669, doi:10.1029/98JD01639, 1998.

Kim, H. S., Y. H. Kim, K. M. Han, J. Kim, and C. H. Song: Ozone production efficiency of a ship-plume: ITCT 2K2 case study, Chemosphere, 143, 17-23, 2016.

Kleinman, L.I., P.H Daum, Y.N Lee, G.I. Senum, S.R. Springston, J. Wany, C. Berkowitz, J. Hubbe, R.A. Zaveri, F.J. Brechtel, J. Jayne, T.B. Onasch, and D. Worsnop: Aircraft observations of aerosol composition and ageing in New England and mid-Atlantic states during the summer 2002 New England Air Quality Study field campaign. J. Geophys. Res. Atmos., 112, D09310. doi:10.1029/2006JD007786, 2007.

5 Kleinman, L., Y.-N. Lee, S. R. Springston, L. Nunnermacker, X. Zhou, R. Brown, K. Hallock, P. Klotz, D. Leahy, J. H. Lee, and L. Newman: Ozone formation at a rural site in the southeastern United States, J. Geophys. Res. Atmos., 99(D2), 3469-3482, doi:10.1029/93JD02991, 1994.

Langford, A.O., C.J. Senff , R.J. Alvarez II , J. Brioude, O.R. Cooper, J.S. Holloway, M.Y. Lin, R.D. Marchbanks, R.B. Pierce, S.P. Sandberg, A.M. Weickmann , and E.J. Williams: An overview of the 2013 Las Vegas Ozone Study (LVOS): Impact of
10 stratospheric intrusions and long-range transport on surface air quality, Atmos. Environ. 109 (2015) 305-322, 2015.

Lefohn, A., D. Shadwick, and S. Oltmans: Characterizing changes in surface ozone levels in metropolitan and rural areas in the United States for 1980-2008 and 1994-2008, Atmos. Environ., 44, 5199-5210, 2010.

Lefohn, A., C. Emery, D. Shadwick, H. Wernli, J. Jung, and S. Oltmans: Estimates of background surface ozone mixing ratios in the United States based on model-derived source apportionment, Atmos. Environ., 84, 275-288,
15 doi:10.1016/j.atmosenv.2013.11.033, 2014.

Lin, X., M. Trainer, and S. C. Liu: On the nonlinearity of the tropospheric ozone production., J. Geophys. Res. Atmos., 93(D12), 15879 – 15888, 1988.

Lin, M., A. M. Fiore, O. R. Cooper, L. W. Horowitz, A. O. Langford, H. Levy, B. J. Johnson, V. Naik, S. J. Oltmans, and C. J. Senff: Springtime high surface ozone events over the western United States: Quantifying the role of stratospheric intrusions,
20 J. Geophys. Res. Atmos., 117, D00V22, 2012.

Lin, M., L. W. Horowitz, R. Payton, A. M. Fiore, and G. Tonnesen: U.S. surface ozone trends and extremes from 1980 to 2014: quantifying the roles of rising Asian emissions, domestic controls, wildfires, and climate, Atmos. Chem. Phys., 17, 2943–2970, doi:10.5194/acp-17-2943-2017, 2017.

Liu, S. C., M. Trainer, F. C. Fehsenfeld, D. D. Parrish, E. J. Williams, D. W. Fahey, G. Hubler, and P. C. Murphy: Ozone
25 production in the rural troposphere and the implications for regional and global ozone distributions, J. Geophys. Res., 92(D4), 4191-4207, 1987.

Logan, J.: Tropospheric ozone: seasonal behavior, trends, and anthropogenic influence., J. Geophys. Res., 90(D6), 10463 – 10482, 1985.

McDuffie, E. E., P. M. Edwards, J. B. Gilman, B. M. Lerner, W. P. Dubé, M. Trainer, D. E. Wolfe, W. M. Angevine, J.
30 deGouw, E. J. Williams, A. G. Tevlin, J. G. Murphy, E. V. Fischer, S. McKeen, T. B. Ryerson, J. Peischl, J. S. Holloway, K. Aikin, A. O. Langford, C. J. Senff, R. J. Alvarez II, S. R. Hall, K. O. Lantz and S. S. Brown: Influence of oil and gas emissions on summertime ozone in the Colorado Northern Front Range, J. Geophys. Res. Atmos., 121, 8712-8729, doi:10.1002/2016JD025265, 2016.

Meagher, J., E. Cowling, F. Fehsenfeld, and W. Parkhurst: Ozone formation and transport in southeastern United States: overview of the SOS Nashville/Middle Tennessee Study, J. Geophys.Res., 103, 22,213-22,223, 1998.

National Research Council: Rethinking the Ozone Problem in Urban and Regional Air Pollution, National Academy Press, Washington, D.C., 489 pp., 1991.

5   NARSTO: An Assessment of Tropospheric Ozone Pollution, Report 1000040, NARSTO, Pasco, WA (also available from EPRI, Palo Alto, CA), 2000.

Naja, M., H. Akimoto, and J. Staehelin: Ozone in background and photochemically aged air over central Europe: Analysis of long-term ozonesonde data from Hohenpeissenberg and Payerne, J. Geophys. Res., 108(D2), 4063, doi:10.1029/2002JD002477, 2003.

10   National Oceanic and Atmospheric Administration (NOAA): ESRL/GMD FTP Data Finder, ftp://aftp.cmdl.noaa.gov/data/ozwv/Ozonesonde/Huntsville,%20Alabama/100%20Meter%20Average%20Files/ html (last access October 2, 2017), 2017.

Newchurch, M., M. Ayoub, S. Oltmans, B. Johnson, and F. Schmidlin: Vertical distributions of ozone at four sites in the United States. J. Geophys. Res. 208 (D1), 4031, doi:10.1029/2002JD002059, 2003.

15   Neuman, J. A., J. B. Nowak, W. Zheng, F. Flocke, T. B. Ryerson, M. Trainer, J. S. Holloway, D. D. Parrish, G. J. Frost, J. Peischl, E. L. Atlas, R. Bahreini, A. G. Wollny, and F. C. Fehsenfeld: Relationship between photochemical ozone production and NO_x oxidation in Houston, Texas, J. Geophys. Res. Atmos, 114, D00F08, doi:10.1029/2008JD011688, 2009.

Neuman, J. A., M. Trainer, S. S. Brown, K.-E. Min, J. B. Nowak, D. D. Parrish, J. Peischl, I. B. Pollack, J. M. Roberts, T. B. Ryerson, and P. R. Veres: HONO emission and production determined from airborne measurements over the Southeast U.S.,

20   J. Geophys. Res. Atmos., 121, 9237–9250, doi:10.1002/2016JD025197, 2016.

Nunnermacker, L. J., D. Imre, P. H. Daum, L. Kleinman, Y.-N. Lee, J. H. Lee, S. R. Springston, L. Newman, J. Weinstein-Lloyd, W. T. Luke, R. Banta, R. Alvarez, C. Senff, S. Sillman, M. Holdren, G. W. Keigley, and X. Zhou: Characterization of the Nashville urban plume on July 3 and July 18, 1995, J. Geophys. Res. Atmos., 103(D21), 28129-28148, doi:10.1029/98JD01961, 1998.

25   Oltmans, S., A. Lefohn, J. Harris, and D. Shadwick: Background ozone levels of air entering the west coast of the US and assessment of longer-term changes, Atmos. Environ., 42, 6020-6038, 2008.

Oltmans, S., A. Lefohn, D. Shadwick, J. Harris, H. Scheel, I. Galbally, D. Tarasick, B. Johnson, E. Brunke, H. Claude, G. Zeng, S. Nichol, F. Schmidlin, J. Davies, E. Cuevas, A. Redondas, H. Naoe, T. Kakano, and T. Kawasato: Recent tropospheric ozone changes – a pattern dominated by slow or no growth, Atmos. Environ., 67, 331-351, 2013.

30   Ordóñez, C., D. Brunner, J. Staehelin, P. Hadjinicolaou, J. A. Pyle, M. Jonas, H. Wernli, and A. S. H. Prévôt: Strong influence of lowermost stratospheric ozone on lower tropospheric background ozone changes over Europe, Geophys. Res. Let., 34, L07805, doi:10.1029/2006GL029113, 2007.

Paoletti, E., A. De Marco, D. C. S. Beddows, R. M. Harrison, and W. J. Manning: Ozone levels in European and USA cities are increasing more than at rural sites, while peak values are decreasing, Environmental Pollution, 192, 295-299, 2014.

Parrish, D. D., L. M. Young, M. H. Newman, K. C. Aikin, and T. B. Ryerson: Ozone design values in Southern California's air basins: Temporal evolution and U.S. background contribution, J. Geophys. Res. 122, 11,166–11,182, doi.org/10.1002/2016JD026329, 2017a.

Parrish, D. D., I. Petropavlovskikh, and S. J. Oltmans: Reversal of long-term trend in baseline ozone concentrations at the North American West Coast, Geophys. Res. Let., 44, 10,675–10,681, doi.org/10.1002/2017GL074960, 2017b.

Pollack, I., T. Ryerson, M. Trainer, J. Neuman, J. Roberts, and D. Parrish: Trends in ozone its precursors and related secondary oxidation products in Los Angeles, California: a synthesis of measurements from 1960-2010, J. Geophys. Res. Atmos., 118, 5891-5911, 2013.

Reynolds, S., C. L. Blanchard, and S. Ziman: Understanding the effectiveness of precursor reductions in lowering 8-hour ozone mixing ratios, J. Air & Waste Manage. Assoc., 53, 195-205, 2003.

Reynolds, S., C. L. Blanchard, and S. Ziman: Understanding the effectiveness of precursor reductions in lowering the 8-hr. O_3 concentration: part II-eastern United States, J. Air & Waste Manage. Assoc., 54, 1452-1470, 2004.

Ryerson, T. B., A. E. Andrews, W. M. Angevine, T. S. Bates, C. A. Brock, B. Cairns, R. C. Cohen, O. R. Cooper, J. A. de Gouw, F. C. Fehsenfeld, R. A. Ferrare, M. L. Fischer, R. C. Flagan, A. H. Goldstein, J. W. Hair, R. M. Hardesty, C. A. Hostetler, J. L. Jimenez, A. O. Langford, E. McCauley, S. A. McKeen, L. T. Molina, A. Nenes, S. J. Oltmans, D. D. Parrish, J. R. Pederson, R. B. Pierce, K. Prather, P. K. Quinn, J. H. Seinfeld, C. J. Senff, A. Sorooshian, J. Stutz, J. D. Surratt, M. Trainer, R. Volkamer, E. J. Williams, and S. C. Wofsy: The 2010 California Research at the Nexus of Air Quality and Climate Change (CalNex) field study, J. Geophys. Res. Atmos., 118, 5830–5866, doi:10.1002/jgrd.50331, 2013.

Saylor, R. D., E. S. Edgerton, B. E. Hartsell, K. Baumann, and D. A. Hansen: Continuous gaseous and total ammonia measurements from the southeastern aerosol research and characterization (SEARCH) study, Atmos. Environ., 44, 4994-5004, 2010.

Schere, K. and G. M. Hidy: Foreword: NARSTO critical reviews., Atmos. Environ., 34, 1853 – 1860, 2000.

Schnell, R. C., S. J. Oltmans, R. R. Neely, M. S. Endres, J. V. Molenar, and A. B. White: Rapid photochemical production of ozone at high concentrations in a rural site during winter, Nature Geoscience, 2 (2), 120-122, doi:10.1038/ngeo415, 2009.

Seigneur, C. and R. Dennis: Atmospheric modeling, in Hidy, G. M., J. R. Brook, K. L. Demerjian, Luisa T. Molina, W.T. Pennell, and R. D. Scheffe, eds., Technical Challenges of Multipollutant Air Quality Management, Springer, New York, 2011.

Seinfeld, J. H.: Atmospheric Chemistry and Physics of Air Pollution, John Wiley and Sons, New York, 1986.

Sillman, S., D. He, M. Pippin, P. H. Daum, D. G. Imre, L. I. Kleinman, and J. H. Lee: Model correlations for ozone, reactive nitrogen, and peroxides for Nashville in comparison with measurements: Implications for O_3-NO_x-hydrocarbon chemistry, J. Geophys. Res. Atmos., 103(D17), 22629-22644, 1998.

Simon, H., A. Reff, B. Wells, J. Xing, and N. Frank: Ozone trends across the United States over a period of decreasing NO_x and VOC emissions, Environ. Sci. Technol., 49(1), 186-195, http://pubs.acs.org/doi/pdf/10.1021/es504514z, 2015.

Singh, H. B. and P. L. Hanst: Peroxyacetyl nitrate (PAN) in the unpolluted atmosphere: an important reservoir for nitrogen oxides, Geophys. Res. Let., 8, 941 – 944, 1981.

Singh, H.: Reactive nitrogen in the troposphere: chemistry and transport of NO_x and PAN, Environ. Sci. & Technol., 21, 320 – 327, 1987.

Solberg, S., R. G. Derwent, Ø. Hov, J. Langner, and A. Lindskog: European abatement of surface ozone in a global perspective, Ambio, 34(1): 47 – 53, doi.org/10.1579/0044-7447-34.1.47, 2005.

5   Solomon, P., Cowling, E., Hidy, G. and C. Furness: Comparison of scientific findings from major ozone field studies in North America and Europe. Atmos. Environ. 34. 1885-1920, 2000.

St. John, J. C., W. L. Chameides, and R. Saylor: Role of anthropogenic NO_x and VOC as ozone precursors: A case study from the SOS Nashville/Middle Tennessee Ozone Study, J. Geophys. Res. Atmos., 103(D17), 22415-22423, 1998.

Starn, T. K., P. B. Shepson, S. B. Bertman, J. S. White, B. G. Splawn, D. D. Riemer, R. G. Zika, K. Olszyna: Observations of
10   isoprene chemistry and its role in ozone production at a semirural site during the 1995 Southern Oxidants Study, J. Geophys. Res., 103, 22425–22435, doi: 1 0.1029/98JD01279, 1998.

Trainer, M., D. D. Parrish, M. P.,Buhr, R. Norton, F. Fehsenfeld, K. Anlauf, J. Bottenheim, Y. Tang, H. Weibe, J. Roberts, R. Tanner, L. Newman, V. Bowersox, J. Meagher, K. Olszyna, M. Rodgers, T. Wang, H. Berresheim, K. Demerjian, and U. Roychowdhury: Correlation of ozone with NO_y in photochemically aged air, J. Geophys. Res. Atmos., 98(D2), 2917 – 2925,
15   1993.

Trainer, M., B. A. Ridley, M. P. Buhr, G. Kok, J. Walega, G. Hübler, D. D. Parrish, and F. C. Fehsenfeld: Regional ozone and urban plumes in the southeastern United States: Birmingham, A case study, J. Geophys. Res. Atmos., 100(D9), 18823- 18834, doi:10.1029/95JD01641, 1995.

Trainer, M., D. Parrish, P. Goldan, P., J. Roberts, and F. Fehsenfeld: Review of observation-based analysis of regional factors
20   influencing ozone concentration, Atmos. Environ., 34, 2045-2062, 2000.

Travis, K. R., D. J. Jacob, J. A. Fisher, P. S. Kim, E. A. Marais, L. Zhu, K. Yu, C. C. Miller, R. M. Yantosca, M. P. Sulprizio, A. M. Thompson, P. O. Wennberg, J. D. Crounse, J. M. St. Clair, R. C. Cohen, J. L. Laughner, J. E. Dibb, S. R. Hall, K. Ullmann, G. M. Wolfe, I. B. Pollack, J. Peischl, J. A. Neuman, and X. Zhou: Why do models overestimate surface ozone in the Southeast United States?, Atmos. Chem. Phys., doi:10.5194/acp-16-13561-2016, 2016.

25   University   of   Alabama   Huntsville   (UAH).   2017.   Huntsville   ozonesonde   station. http://www.nsstc.uah.edu/atmchem/about_ozonesonde.html (last access October 2, 2017), 2017.U. S. EPA: Regional and Seasonal   Analysis   of   North   American   Background   Ozone   Estimated   from   Two   Studies, http://www.epa.gov/ttn/naaqs/standards/ozone/data/20120814 Background Ozone.pdf (accessed January 2015), 2012.

U.S.   EPA: Health   Risk   and   Exposure   Assessment   for   Ozone   Final   Report,   EPA-452/R-14-004a,
30   http://www.epa.gov/ttn/naaqs/standards/ozone/data/20140829healthrea.pdf, (last access August 19, 2015), 2014.

U.S. EPA: Ozone (O_3) Standards - Documents from Current Review - Risk and Exposure Assessments, http://www.epa.gov/ttn/naaqs/standards/ozone/s_o3_2008_rea.html (last access August 19, 2015), 2015a.

U.S.   EPA: Ozone   (O_3)   Standards   -   Table   of   Historical   Ozone   NAAQS, http://www.epa.gov/ttn/naaqs/standards/ozone/s_o3_history.html (last access August 19, 2015), 2015b.

U.S. EPA: Environmental Protection Agency 40 CFR Parts 50, 51, 52, 53 and 58 [EPA-HQ-OAR-2008-0699; FRL-9918-43-OAR] RIN 2060-AP38, National Ambient Air Quality Standards for Ozone, http://www.epa.gov/airquality/ozonepollution/pdfs/20141125proposal.pdf (last access August 19, 2015), 2015c.

U.S. EPA: National Trends in Ozone Levels, http://www.epa.gov/airtrends/ozone.html (last access August 19, 2015), 2015d.

U.S. EPA: Air Quality Trends, http://www.epa.gov/airtrends/aqtrends.html#comparison (last access August 19, 2015), 2015e.

U.S. EPA: AirData: Download Data Files. http://aqsdr1.epa.gov/aqsweb/aqstmp/airdata/download_files.html (last access March 15, 2017), 2016a.

U.S. EPA: Clean Air Status and Trends Network (CASTNET). https://www.epa.gov/castnet (last access March 24, 2016), 2016b.

U.S. EPA: Air Markets Program Data. http://ampd.epa.gov/ampd/ (last access September 12, 2016), 2016c.

U.S. EPA: Air Pollutant Emission Trends Data. https://www.epa.gov/air-emissions-inventories/air-pollutant-emissions-trends-data (last access September 25, 2016), 2016d.

Warneke, C., M. Trainer, J. A. de Gouw, et al.: Instrumentation and measurement strategy for the NOAA SENEX aircraft campaign as part of the Southeast Atmosphere Study 2013, Atmos. Meas. Tech., 9, 3063-3093, doi:10.5194/amt-2015-388, 2016.

Wiedinmyer, C., X. Tie, A. Guenther, R. Neilson, and C. Granier: Future changes in biogenic isoprene emissions: how might they affect regional and global atmospheric chemistry?, Earth Interactions, 10, https://doi.org/10.1175/EI174.1, 2006.

Williams, E. J., K. Baumann, J. M. Roberts, S. B. Bertman, R. B. Norton, F. C. Fehsenfeld, S. R. Springston, L. J. Nunnermacker, L. Newman, K. Olszyna, J. Meagher, B. Hartsell, E. Edgerton, J. R. Pearson, and M. O. Rodgers: Intercomparison of ground-based NO_y measurement techniques, J. Geophys. Res. 103 (D17), 22261–22280, 1998.

Wilson, R. C., Z. L. Fleming, P. S. Monks, G. Clain, S. Henne, I. B. Konovalov, S. Szopa, and L. Menut: Have primary emission reduction measures reduced ozone across Europe? An analysis of European rural background ozone trends 1996–2005, Atmos. Chem. Phys., 12, 437–454, doi:10.5194/acp-12-437-2012, 2012.

Zaveri, R. A., C. M. Berkowitz, L. I. Kleinman, S. R. Springston, P. V. Doskey, W. A. Lonneman, and C. W. Spicer: Ozone production efficiency and NO_x depletion in an urban plume: Interpretation of field observations and implications for evaluating O_3-NO_x-VOC sensitivity, J. Geophys. Res. Atmos., 108 (D14), doi:10.1029/2002JD003144, 2003.

Zhang, L., D. J. Jacob, N. V. Downey, D. A. Wood, D. Blewitt, C. C. Carouge, A. van Donkelaar, D. B. A. Jones, L. T. Murray, and Y. Wang: Improved estimate of the policy-relevant background ozone in the United States using the GEOS-Chem global model with $1/2° \times 2/3°$ horizontal resolution over North America, Atmos. Environ., 45 (37), 6769 – 6776, doi.org/10.1016/j.atmosenv.2011.07.054, 2011.
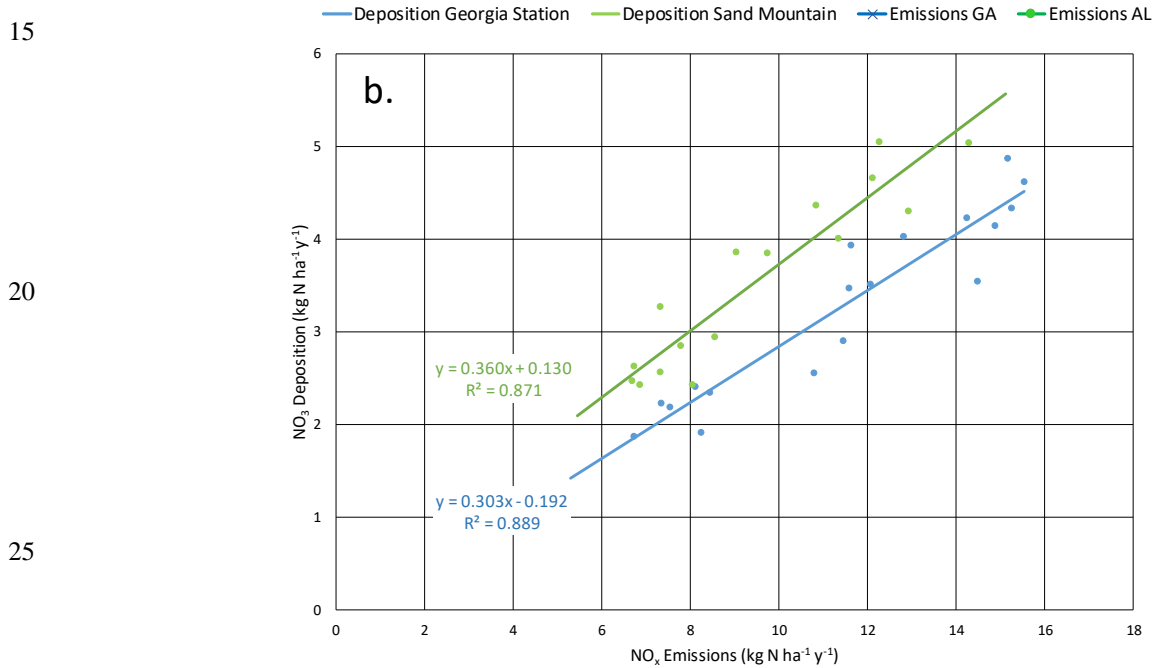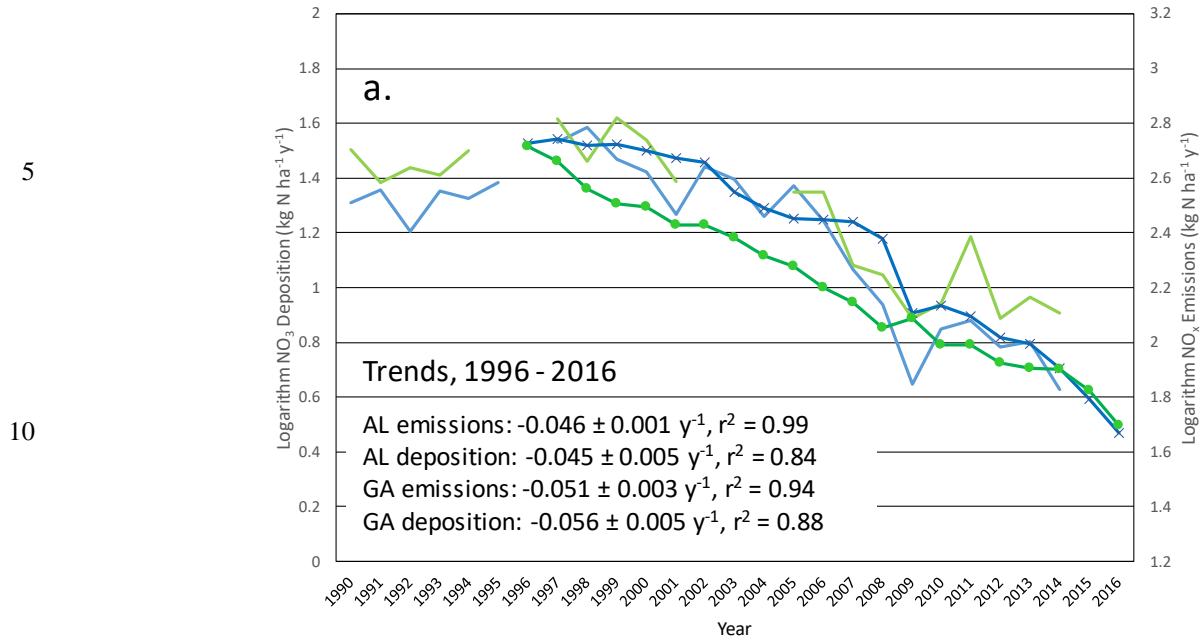
Figure 1. Comparison of nitrate deposition (wet plus dry) to NO$_x$ emission densities in Georgia and Alabama as (a) temporal trends and (b) regression of deposition against emissions (with same color coding in both panels). Nitrate deposition and NO$_x$ emission densities are expressed as kg ha^{-1} y^{-1}. NO$_x$ emissions are from all source sectors (supplement). Panel (a) shows natural logarithms vs. year and indicates that emissions and deposition trended downward at the same rates. Panel (b) slopes are statistically significant (p < 0.0001) and intercepts are not (p > 0.1).
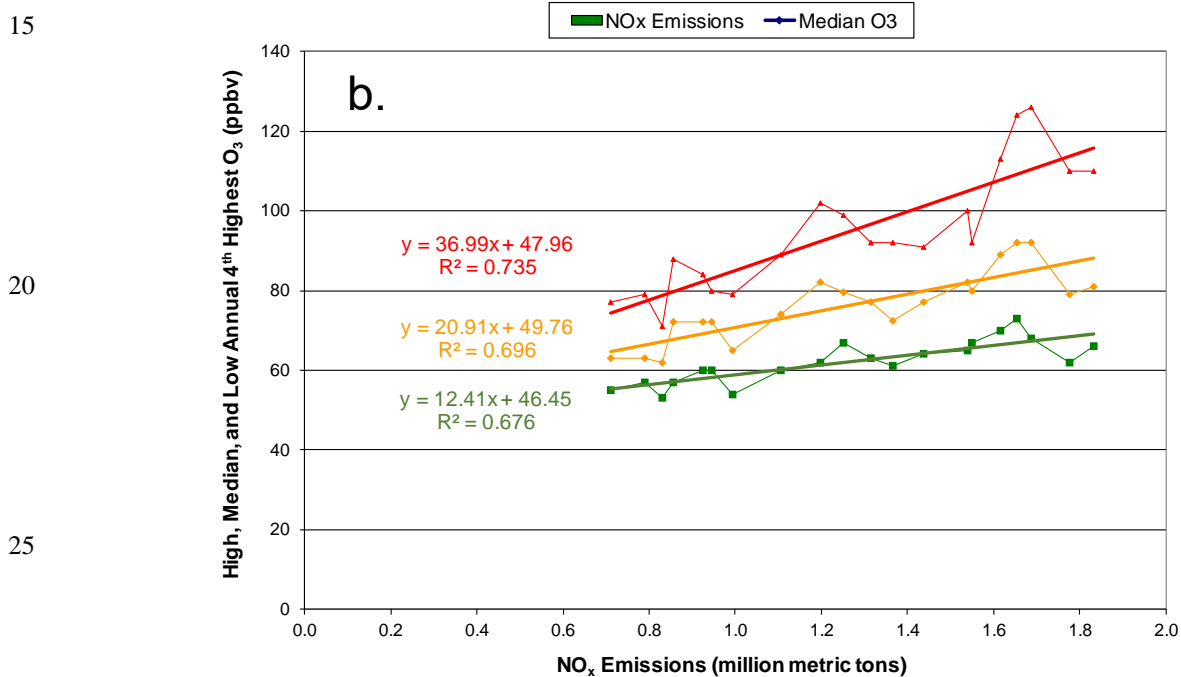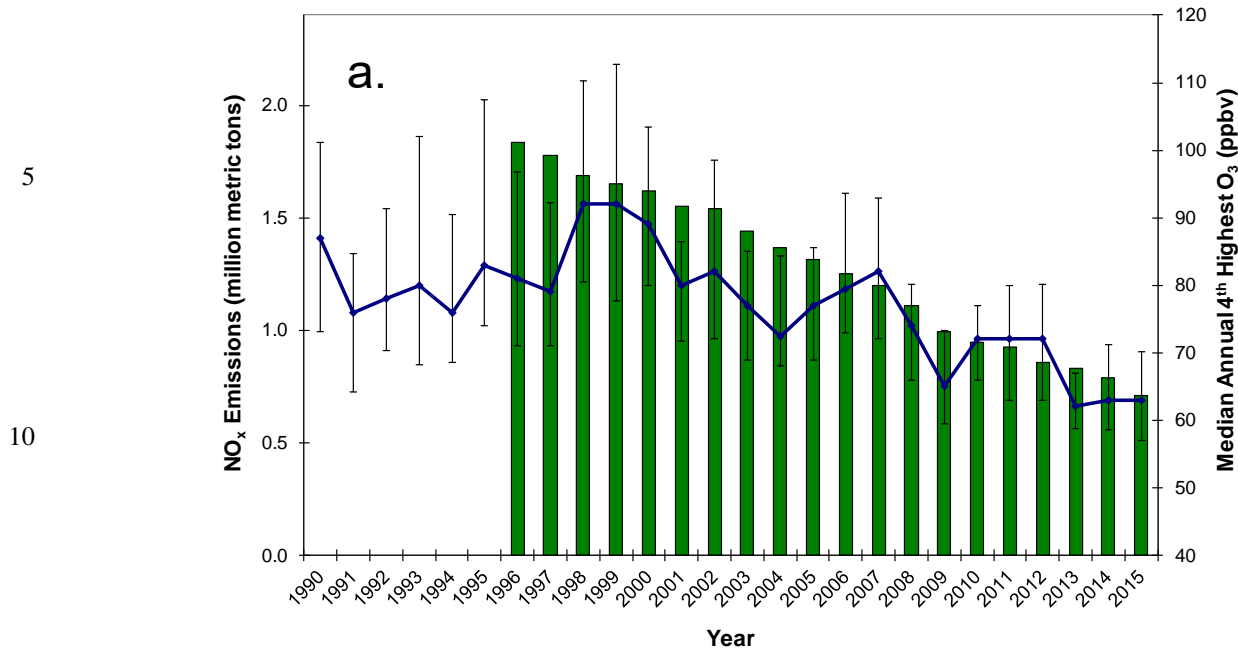
Figure 2. Comparison of annual 4th-highest daily peak 8-hour O₃ to NO$_x$ emissions in Georgia and Alabama (a) trends (± 90th and 10th percentile sites) and (b) regressions (high = 90th percentile site, median, and low = 10th percentile site annual 4th-highest daily peak 8-hour O₃). NO$_x$ emissions are from all source sectors (supplement). O₃ data include all EPA AQS monitors in Georgia and Alabama for each year having at least 75% data completeness (mean = 55 monitors, low of 32 – 36 in 1990 – 1993). Slopes and intercepts are statistically significant (p < 0.0001).
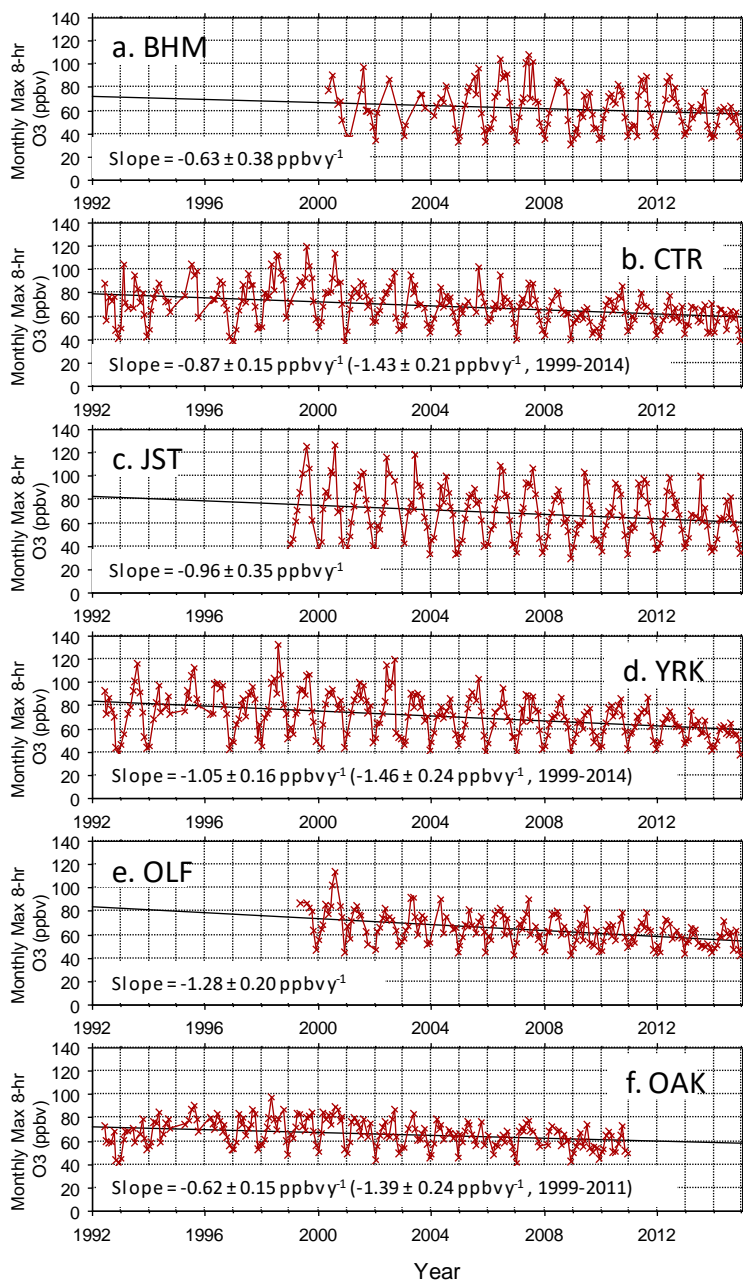
Figure 3. Monthly maxima of daily peak 8-hour average O₃ mixing ratios. All monthly maxima are determined from 24 or more days with 18 or more sampling hours per day. PNS and GFP (not shown) exhibit trends of -1.64 ± 0.45 and -0.60 ± 0.32 ppbv y⁻¹, respectively. Trends are statistically significant (p < 0.01) at CTR, JST, OAK, OLF, PNS, and YRK.
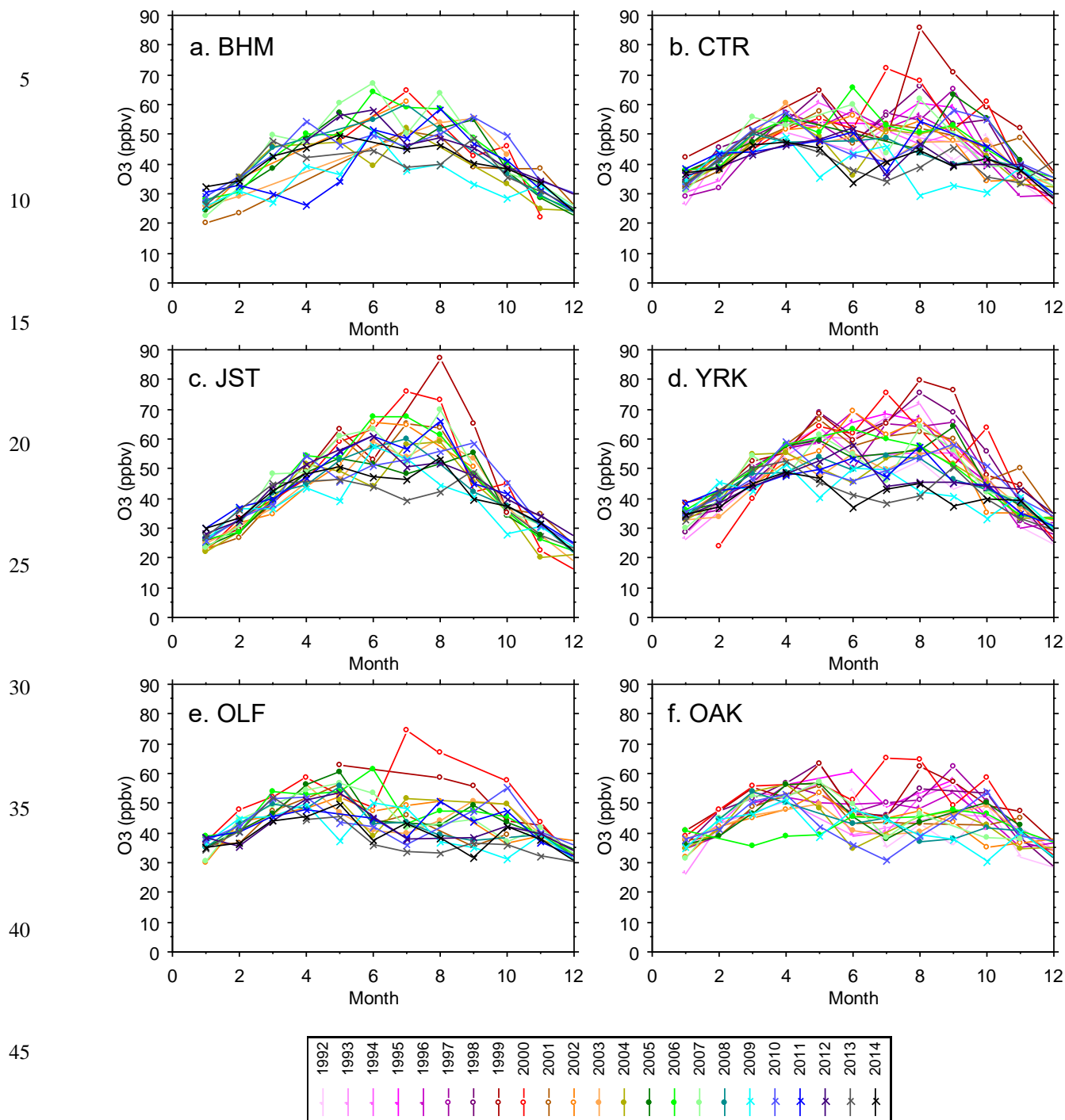
Figure 4. Monthly means of daily peak 8-hour average O₃ mixing ratios. All monthly means are determined from 24 or more days with 18 or more sampling hours per day. Standard errors of the means average 2 (range 0.8 – 5) ppbv.
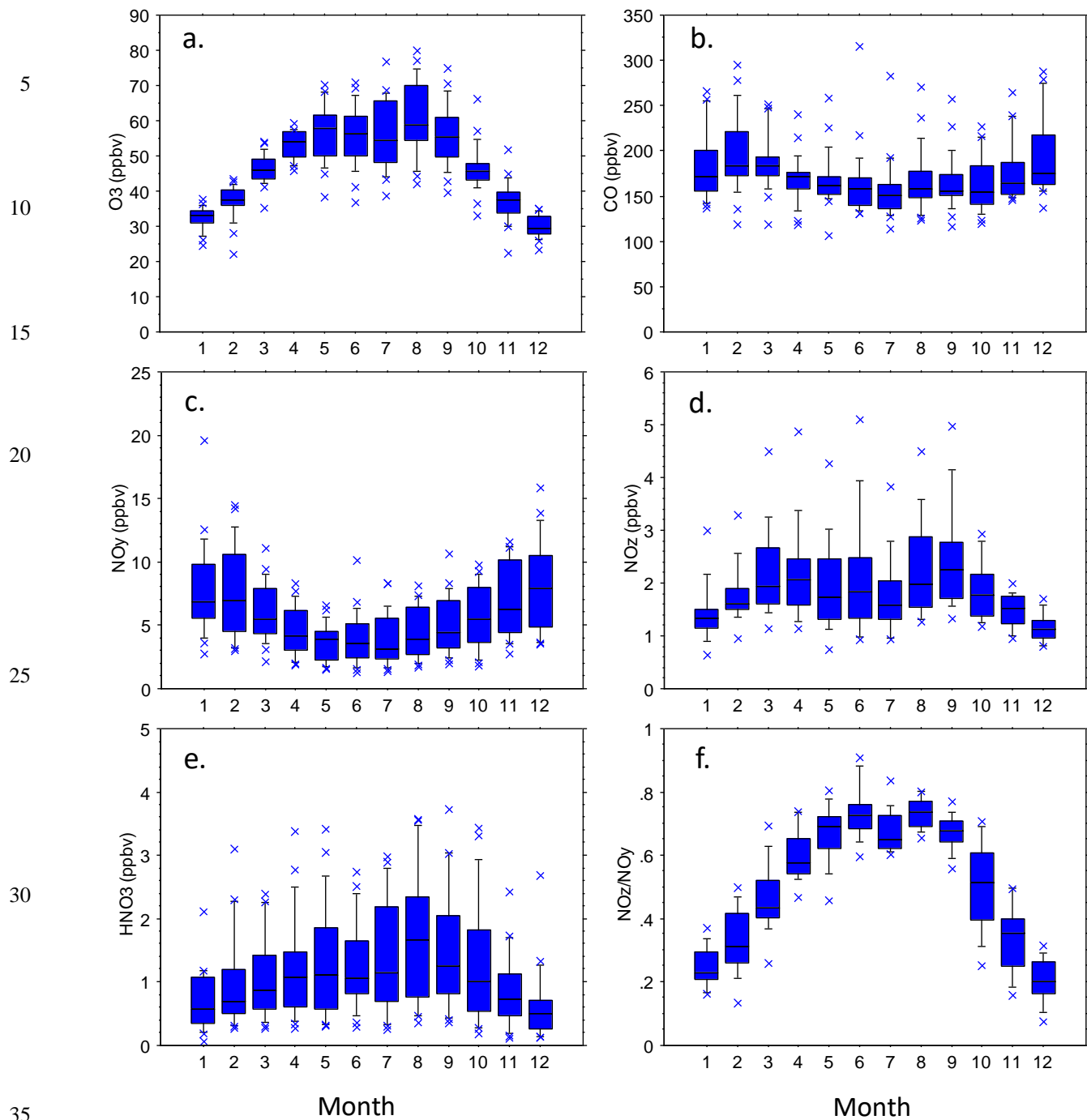
Figure 5. Statistical distributions of mean monthly species mixing ratios, all SEARCH sites, 1992 – 2014. Distributions indicate the 10th, 25th, 50th, 75th, and 90th percentiles of the monthly averages.
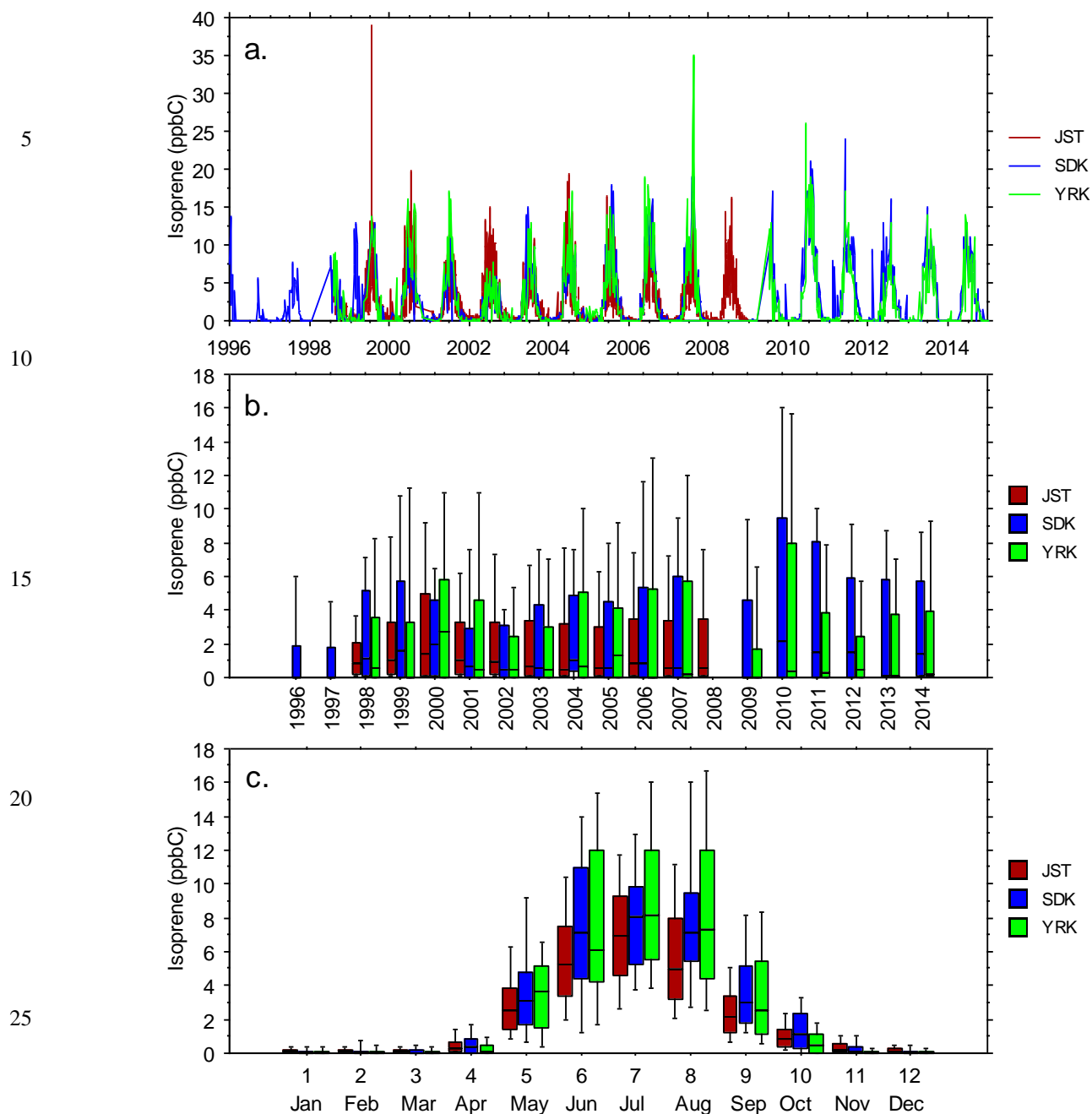
Figure 6. (a) Daily-average isoprene mixing ratios vs. date, (b) statistical distributions of daily-average isoprene mixing ratios vs. year, and (c) statistical distributions of daily-average isoprene mixing ratios vs. month. Samples were obtained every day at JST and once every six days at YRK and SDK (Blanchard et al., 2010). Distributions indicate the 10th, 25th, 50th, 75th, and 90th percentiles.
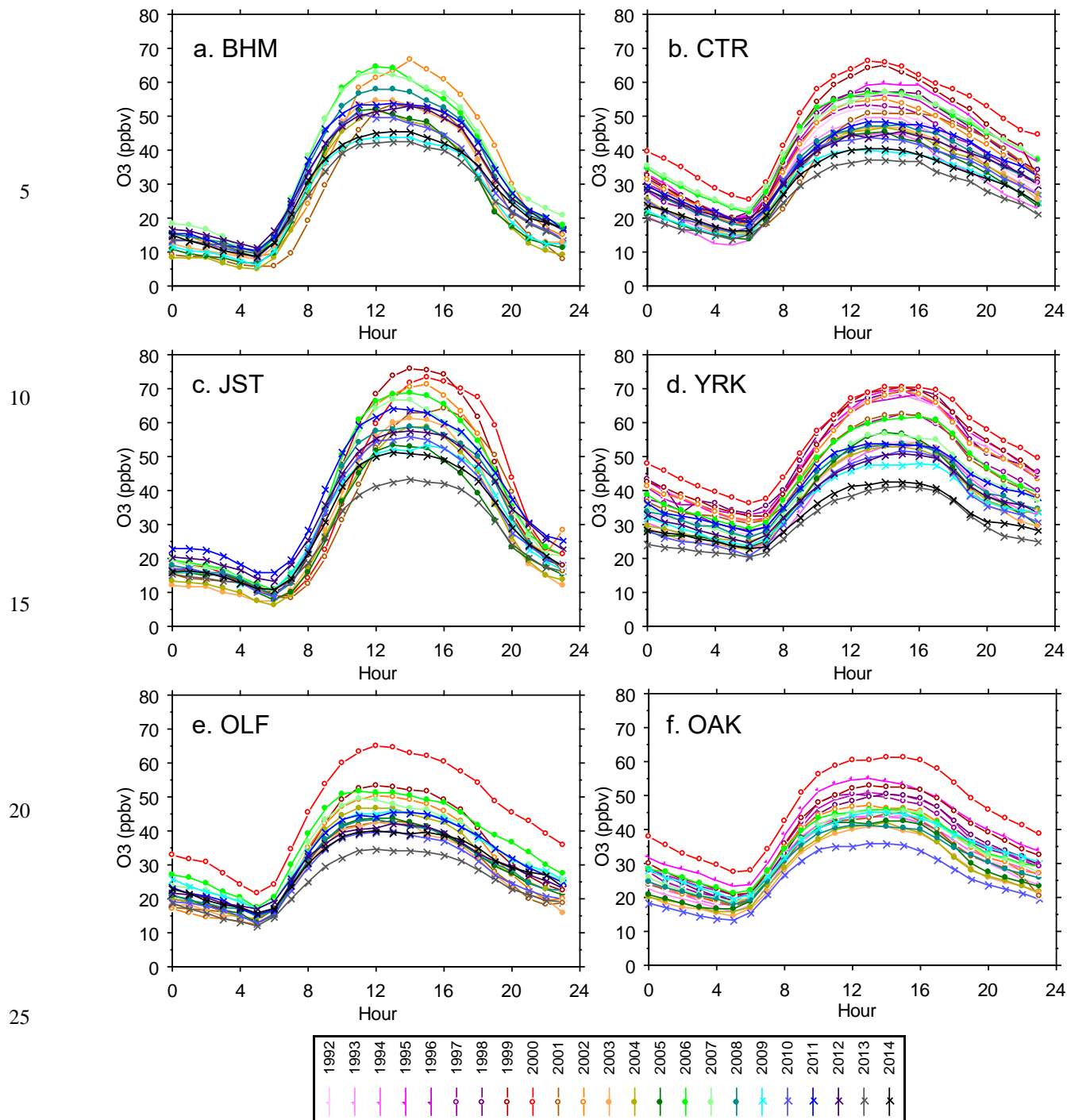
Figure 7. Average O₃ mixing ratios vs. hour, by year. Each data point is the mean of all hourly measurements during June through August. Sites at PNS and GFP (not shown) exhibit similar diurnal profiles and trends (sampling at those sites ended after 2009 and 2012, respectively). Standard errors of the means are 0.3 – 4 ppbv, ~2% of mean O₃ mixing ratios.
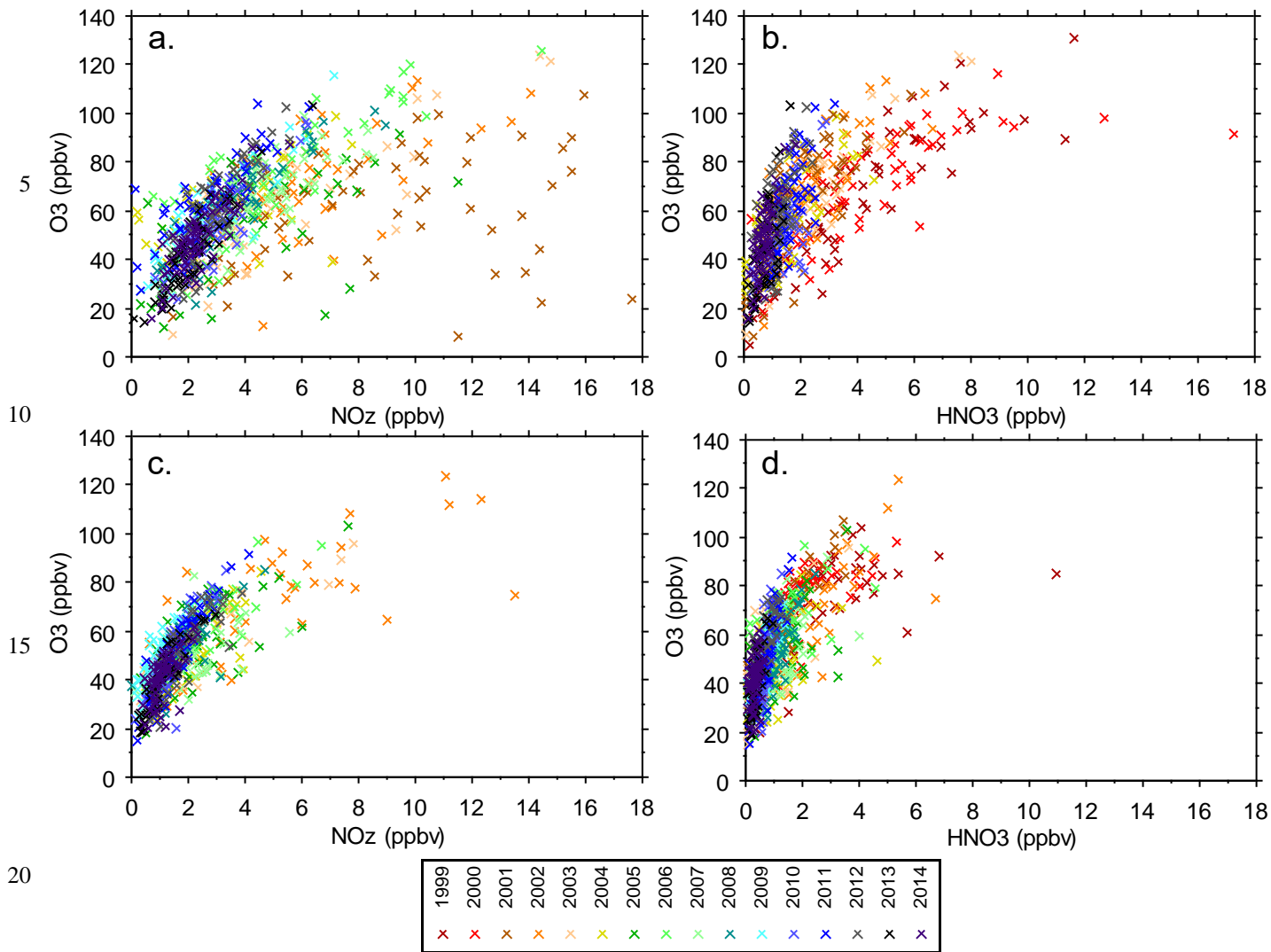
Figure 8. (a) O_3 vs. NO_z at JST; (b) O_3 vs. HNO_3 at JST; (c) O_3 vs. NO_z at YRK; and (d) O_3 vs. HNO_3 at YRK. Each point is the 2 – 3 p.m. hourly average on one day, limited to days in June or July and delineated by year. The 2001 and 2002 NO_z data may be biased high due to lower NO_2 mixing ratios obtained by the instrumentation used at that time (Figure S2).

O3 (ppbv) = 20.84 + 13.05 * NOz (ppbv); R^2 = .7
O3 (ppbv) = 23.97 + 12.15 * NOz (ppbv); R^2 = .5 (Favorable)

O3 (ppbv) = 16.46 + 25.73 * NOz (ppbv); R^2 = .61
O3 (ppbv) = 16.38 + 25.8 * NOz (ppbv); R^2 = .53 (Favorable)

O3 (ppbv) = 11.37 + 14.82 * NOz (ppbv); R^2 = .84
O3 (ppbv) = 11.53 + 14.48 * NOz (ppbv); R^2 = .82 (Favorable)

O3 (ppbv) = 19.47 + 18.78 * NOz (ppbv); R^2 = .81
O3 (ppbv) = 21.71 + 17.6 * NOz (ppbv); R^2 = .75 (Favorable)
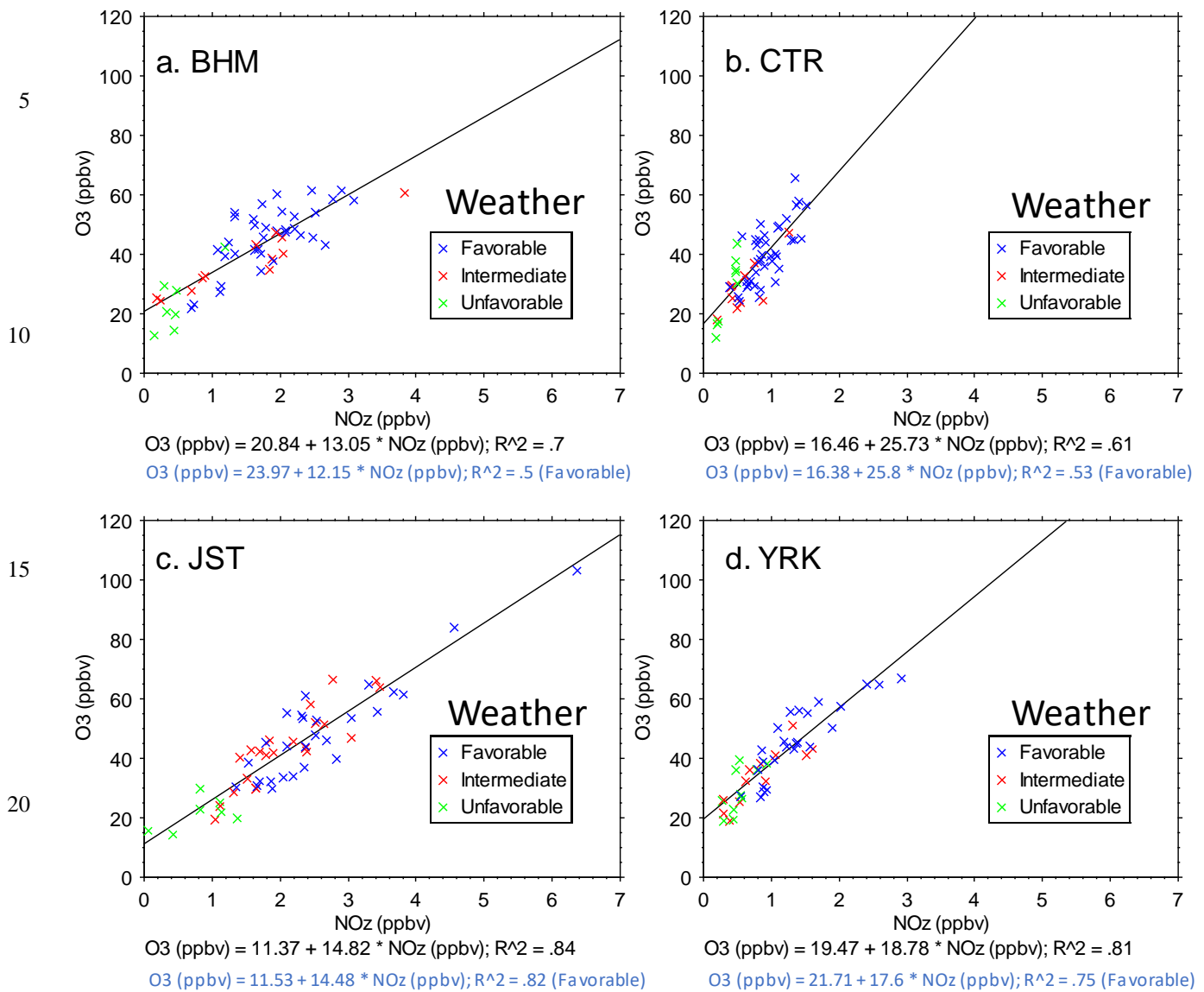
Figure 9. O_3 vs. NO_z during June and July, 2013. Each point is the 2 – 3 p.m. hourly average on one day. The data were selected to represent the approximate mid-point of the mid-day O_3 maxima and to span a period around the summer solstice (- ~20 days, + ~40 days) when solar radiation is highest on average. The regression slopes show higher rural than urban values: BHM = 13.05 ± 1.19 ppbv ppbv^{-1}, JST = 14.82 ± 0.88 ppbv ppbv^{-1}, YRK = 18.78 ± 1.38 ppbv ppbv^{-1}, CTR = 25.73 ± 2.76 ppbv ppbv^{-1}. Corresponding regression slopes for O_x vs. NO_z are: BHM = 12.00 ± 1.16 ppbv ppbv^{-1}, JST = 13.88 ± 0.93 ppbv ppbv^{-1}, YRK = 18.85 ± 1.37 ppbv ppbv^{-1}, CTR = 25.79 ± 2.79 ppbv ppbv^{-1}. Symbols indicate the favorability of weather to O_3 formation and accumulation: (1) favorable = T > 25°C, RH < 70%, and solar radiation > 500 W m^{-2}, (2) intermediate = neither favorable nor unfavorable, (3) unfavorable = T < 25°C, RH > 70%, and solar radiation < 500 W m^{-2}. Regression results are shown for all days and for the days with favorable weather.
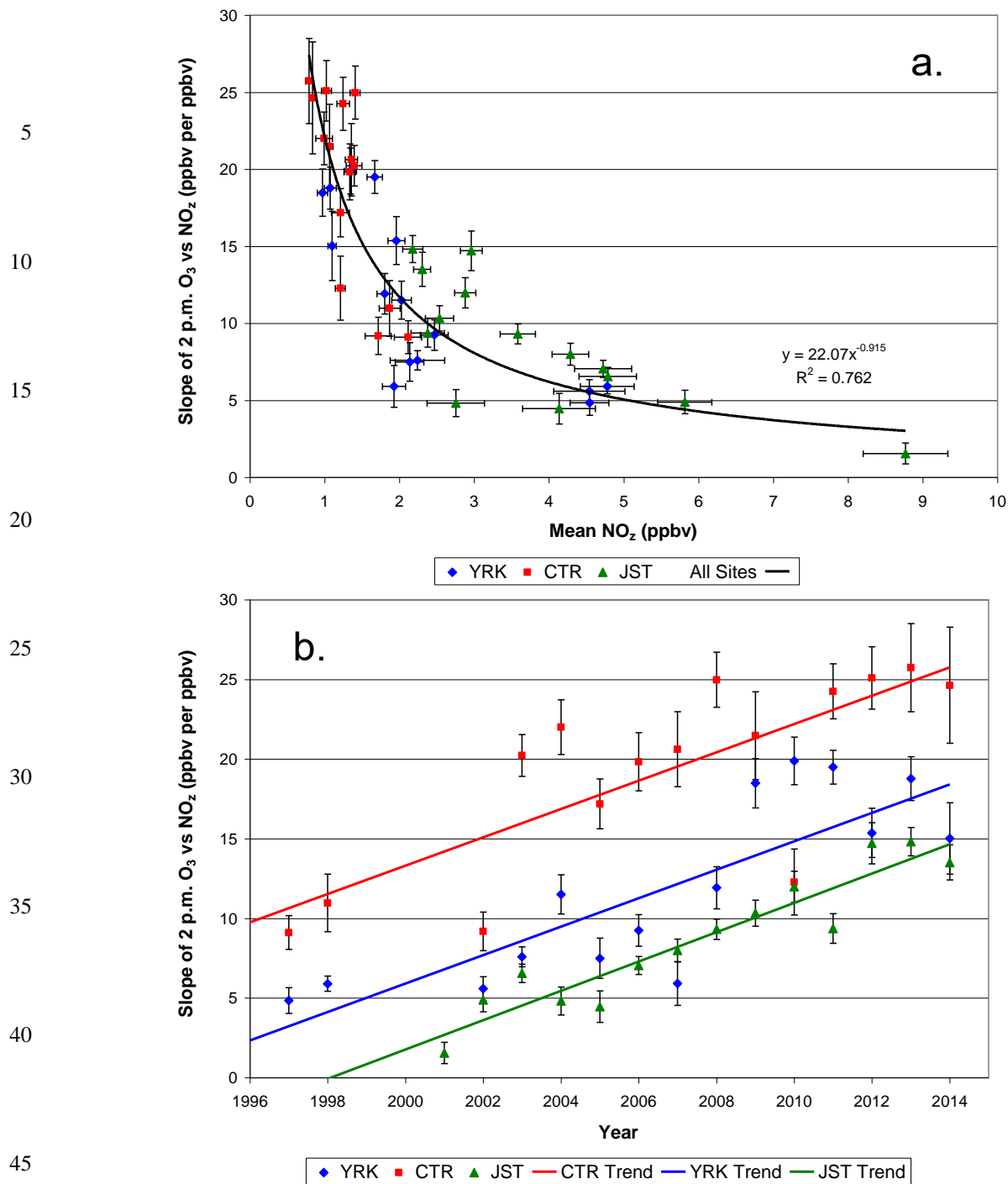
Figure 10. (a) Summer CTR, JST, and YRK slope of daily (2 p.m.) O₃ and NOz vs. mean (2 p.m.) NOz mixing ratios, and (b) summer regression slope vs. year. NO₂ data were not available for 1999 through 2001. Vertical and horizontal error bars are one standard error of the regression slopes and one standard error of the NOz means, respectively. Mean NOz measurement uncertainty is estimated as 0.2 ppbv (1 sigma).